The Plant Cell, Vol. 22: 3574–3588, November 2010, www.plantcell.org © 2010 American Society of Plant Biologists

TCP Transcription Factors Regulate the Activities of ASYMMETRIC LEAVES1 and miR164, as Well as the Auxin Response, during Differentiation of Leaves in *Arabidopsis* [C][W]

Tomotsugu Koyama,[a,1] Nobutaka Mitsuda,[b] Motoaki Seki,[c] Kazuo Shinozaki,[d] and Masaru Ohme-Takagi[b]

[a] Division of Integrated Life Science, Graduate School of Biostudies, Kyoto University, Oiwakecho, Kitashirakawa, Sakyo, Kyoto 606-8502, Japan

[b] Bioproduction Research Institute, National Institute of Advanced Industrial Science and Technology, Tsukuba, Ibaraki 305-8562, Japan

[c] Plant Genomic Network Research Team, RIKEN Plant Science Center, Tsurumi-ku, Yokohama, Kanagawa 230-0045, Japan

[d] Gene Discovery Research Group, RIKEN Plant Science Center, Tsurumi-ku, Yokohama, Kanagawa 230-0045, Japan

Coordination of the maintenance of the undifferentiated fate of cells in the shoot meristem and the promotion of cellular differentiation in plant organs is essential for the development of plant shoots. CINCINNATA-like (CIN-like) TEOSINTE BRANCHED1, CYCLOIDEA, and PCF (TCP) transcription factors are involved in this coordination via the negative regulation of *CUP-SHAPED COTYLEDON* (*CUC*) genes, which regulate the formation of shoot meristems and the specification of organ boundaries. However, the molecular mechanism of the action of CIN-like TCPs is poorly understood. We show here that TCP3, a model of CIN-like TCPs of *Arabidopsis thaliana*, directly activates the expression of genes for miR164, ASYMMETRIC LEAVES1 (AS1), INDOLE-3-ACETIC ACID3/SHORT HYPOCOTYL2 (IAA3/SHY2), and SMALL AUXIN UP RNA (SAUR) proteins. Gain of function of these genes suppressed the formation of shoot meristems and resulted in the fusion of cotyledons, whereas their loss of function induced ectopic expression of *CUC* genes in leaves. Our results indicate that miR164, *AS1*, *IAA3*/*SHY2*, and *SAUR* partially but cooperatively suppress the expression of *CUC* genes. Since *CIN*-like *TCP* genes were revealed to act dose dependently in the differentiation of leaves, we propose that evolutionarily diverse CIN-like TCPs have important roles in the signaling pathways that generate different leaf forms, without having any lethal effects on shoots.

INTRODUCTION

The development of seed plants is a continuous process, during which the same types of organs emerge repeatedly throughout each plant's life cycle. Leaves are generated repeatedly from shoot apical meristems (SAMs), each of which maintains a pool of pluripotent stem cells at its center. This reiterative developmental process requires maintenance of a precise balance between populations of undifferentiated and differentiated cells (Weigel and Jürgens 2002; Carraro et al., 2006). The formation and maintenance of the undifferentiated fate of cells in the SAM depends on the actions of KNOTTED1-like HOMEOBOX (KNOX) transcription factors (TFs; Hake et al., 2004; Laux et al., 2004). In leaf primordia, coordination of the promotion of differentiated fates and the elimination of undifferentiated fates is achieved by a complex regulatory network, which involves the actions of plant hormones and the activities of several families of TFs (Tsukaya, 2005; Bowman and Floyd, 2008). *ASYMMETRIC LEAVES1* (*AS1*), *ROUGH SHEATH2*, and *PHANTASTICA*, which encode MYB-domain TFs in *Arabidopsis thaliana*, *Zea mays*, and *Antirrhinum majus*, respectively, have been shown to regulate this network (Waites et al., 1998; Timmermans et al., 1999; Tsiantis et al., 1999; Byrne et al., 2000). The mutation of these *MYB*-like genes inhibits cell differentiation and induces the ectopic expression of *KNOX* genes (Schneeberger et al., 1998; Byrne et al., 2000; Ori et al., 2000; Semiarti et al., 2001). These *MYB*-like genes are specifically expressed in the shoot lateral organs, and their pattern of expression is complementary to that of the *KNOX* genes. AS1 forms a complex with AS2, a LOB-domain TF, and binds to the promoters of *KNOX* genes to repress their transcription (Phelps-Durr et al., 2005; Ueno et al., 2007; Guo et al., 2008).

The coordination of the maintenance of undifferentiated fates in the SAM and the promotion of differentiation of cells in leaves requires the functions of TCPs (Nath et al., 2003; Palatnik et al., 2003; Koyama et al., 2007; Ori et al., 2007; Efroni et al., 2008; Schommer et al., 2008). The *Arabidopsis* genome contains 24 *TCP* genes (Martín-Trillo and Cubas, 2010). However, their roles in the regulation of differentiation have not been well characterized because of their extreme genetic redundancy

[1] Address correspondence to t-koyama@lif.kyoto-u.ac.jp.
The author responsible for distribution of materials integral to the findings presented in this article in accordance with the policy described in the Instructions for Authors (www.plantcell.org) is: Tomotsugu Koyama (t-koyama@lif.kyoto-u.ac.jp).
[C]Some figures in this article are displayed in color online but in black and white in the print edition.
[W]Online version contains Web-only data.
www.plantcell.org/cgi/doi/10.1105/tpc.110.075598

and the complexity of their own regulation, which also involves microRNAs. We demonstrated that the *CINCINNATA*-like (*CIN*-like) *TCP* genes, namely, *TCP2*, *TCP3*, *TCP4*, *TCP5*, *TCP10*, *TCP13*, *TCP17*, and *TCP24*, regulate the differentiation of cells in leaves by generating chimeric TCP repressors, composed of dominant-negative versions of TCPs (TCPSRDXs; Hiratsu et al., 2003; Koyama et al., 2007). Plants that express *TCPSRDX* genes have wavy leaves, irregular vasculature, and undifferentiated cells, with ectopic formation of shoot meristems in cotyledons. The *Arabidopsis jaw-d* mutants, in which the expression of the target genes for *miR319A*/*JAW* (specifically, *TCP2*, *TCP3*, *TCP4*, *TCP10*, and *TCP24*) is suppressed, have a wavy-leaf phenotype (Palatnik et al., 2003). By contrast, ectopic expression of mutated *TCP* genes in which the target sequence for miR319 has been replaced by a nontarget sequence induces defects in the formation of a functional shoot meristem and the fusion of cotyledons (Palatnik et al., 2003; Koyama et al., 2007; Nag et al., 2009). Similar defects were reported in the case of the *lanceolate* (*la*) mutant of tomato (*Solanum lycopersicum*), in which a mutation in a *TCP* gene rendered it resistant to the effects of miR319 (Mathan and Jenkins, 1962; Caruso, 1968; Ori et al., 2007).

We were able to demonstrate that CIN-like TCPs negatively regulate the expression of *CUP-SHAPED COTYLEDON1* (*CUC1*) and *CUC3* by showing that the expression of *TCPSRDX* genes induces the ectopic expression of *CUC* genes in cotyledons and leaves. By contrast, the expression of the miR319-resistant version of *TCP3* suppresses expression of *CUC* genes in the apical domain of shoots (Koyama et al., 2007). *CUC* genes encode NAC TFs and have important roles at boundary regions during the formation of shoot meristems in the axils of leaves and during the separation of organs (Aida et al., 1997; Vroemen et al., 2003; Hibara et al., 2006). Expression of *TCP3SRDX* results in plants that morphologically resemble plants with an excess of active *CUC* genes. The strong and ubiquitous expression of *CUC1* induces the formation of shoot meristems on cotyledons (Hibara et al., 2003). Escape from miR164-mediated downregulation of *CUC2* results in serration of leaf margins and the delayed differentiation of leaves (Nikovics et al., 2006; Larue et al., 2009). Consistent with this observation, the expression of *CIN*-like *TCP* genes is specific to leaves and largely complementary to that of *CUC* genes, which occurs at the boundary regions, except that *CUC2* is also expressed at the serration of leaf margins (Aida et al., 1999; Palatnik et al., 2003; Nikovics et al., 2006; Koyama et al., 2007).

Given that TCP3 is a transcriptional activator, we postulated that TCP3 might act indirectly to regulate the expression of *CUC* genes (Koyama et al., 2007). We showed that the level of expression of miR164, which negatively regulates the expression of *CUC1* and *CUC2*, was reduced by *TCP3SRDX* (Koyama et al., 2007). However, the mechanism of the negative regulation of *CUC* genes by TCP3 is poorly understood. In this study, we showed that CIN-like TCPs directly activate *miR164*, *AS1*, *INDOLE-3-ACETIC ACID3*/*SHORT HYPOCOTYL2* (*IAA3*/*SHY2*), and several auxin-inducible genes and that these target genes of TCPs act as negative regulators of the expression of *CUC* genes. We present a possible model for the regulation of the promotion of leaf differentiation by CIN-like TCPs.

RESULTS

CIN-Like *TCP* Genes Act Dose Dependently in the Development of Leaves and the SAM

Single mutations of individual *CIN*-like *TCP* genes did not, by themselves, generate visibly mutant phenotypes, as a consequence of the redundancy of the respective gene products (Koyama et al., 2007). Therefore, we prepared multiple knockout lines to investigate the contribution of each *CIN*-like *TCP* gene to shoot morphology and the regulation of expression of downstream genes (see Supplemental Figures 1 and 2 online). The double mutants *tcp3 tcp4* and *tcp3 tcp10* had some signs of waving. The triple, quadruple, and quintuple mutants *tcp3 tcp4 tcp10* (*tcp3/4/10*), *tcp3 tcp4 tcp5 tcp10* (*tcp3/4/5/10*), and *tcp3 tcp4 tcp5 tcp10 tcp13* (*tcp3/4/5/10/13*), respectively, exhibited dose-dependent changes in morphology, which included epinasty of cotyledons, excess growth of leaf surfaces, and leaves with wavy margins (Figures 1A and 1B). Moreover, the expression of *miR319A* in the *tcp3/4/5/10/13* mutant (*Pro35S:miR319A tcp3/4/5/10/13*), which suppressed the expression of *TCP2* and *TCP24* in addition to the inactivation of *TCP3/4/5/10/13*, resulted in severely epinastic cotyledons and leaves with extremely wavy margins (Figures 1A and 1B). The cotyledons of *Pro35S:miR319A tcp3/4/5/10/13* plants also had ectopic formation of trichomes and irregular margins (Figures 1A, 1C, and 1D). The vasculature of *Pro35S:miR319A tcp3/4/5/10/13* was disorganized compared with that of the wild type, but it was extended into the marginal outgrowths of the cotyledons (Figures 1C and 1D). The *Pro35S:miR319A tcp3/4/5/10/13* and *tcp3/4/5/10/13* plants occasionally had severe defects in the expansion of leaves (Figures 1E and 1F). The defects were probably caused by inhibition of cellular differentiation because the epidermal cells of wild-type leaves had a pavement-like pattern, whereas those of *tcp3/4/5/10/13* had a rounded shape (Figures 1G and 1H). Furthermore, *tcp3/4/5/10/13* mutants produced more leaves than the wild type before flowering, which was consistent with the report by Palatnik et al. (2003) (see Supplemental Figure 3 online). In contrast with the morphology of the leaves, the SAM of *tcp3/4/10*, *tcp3/4/5/10*, and *tcp3/4/5/10/13* was apparently normal, but that of *Pro35S:miR319A tcp3/4/5/10/13* was disorganized and formed multiple shoots (Figures 1I to 1K). *Pro35S:miR319A tcp3/4/5/10/13* occasionally produced fasciated stems and bushy inflorescences, which were probably caused by the growth of split SAMs and axillary shoots due to a lack of the intact primary meristem (see Supplemental Figure 4 online). These results suggested that *CIN*-like *TCP* genes regulated the development of leaves and the SAM.

By contrast, *Pro35S:mTCP3* plants, in which the miR319-resistant version of *TCP3* (*mTCP3*) was expressed, had a severely abnormal phenotype that failed to develop a functional SAM, as reported previously (Koyama et al., 2007; Figure 1L). *Pro35S:mTCP3* plants with a moderate phenotype produced several leaves with a narrow shape (Figures 1M and 1O). *Pro35S:mTCP3* plants with a mild phenotype developed leaves and the inflorescence (Figures 1N, 1P, and 1R). However, leaves that were produced later in development had smooth margins, whereas those of the wild type had serrations in the margin

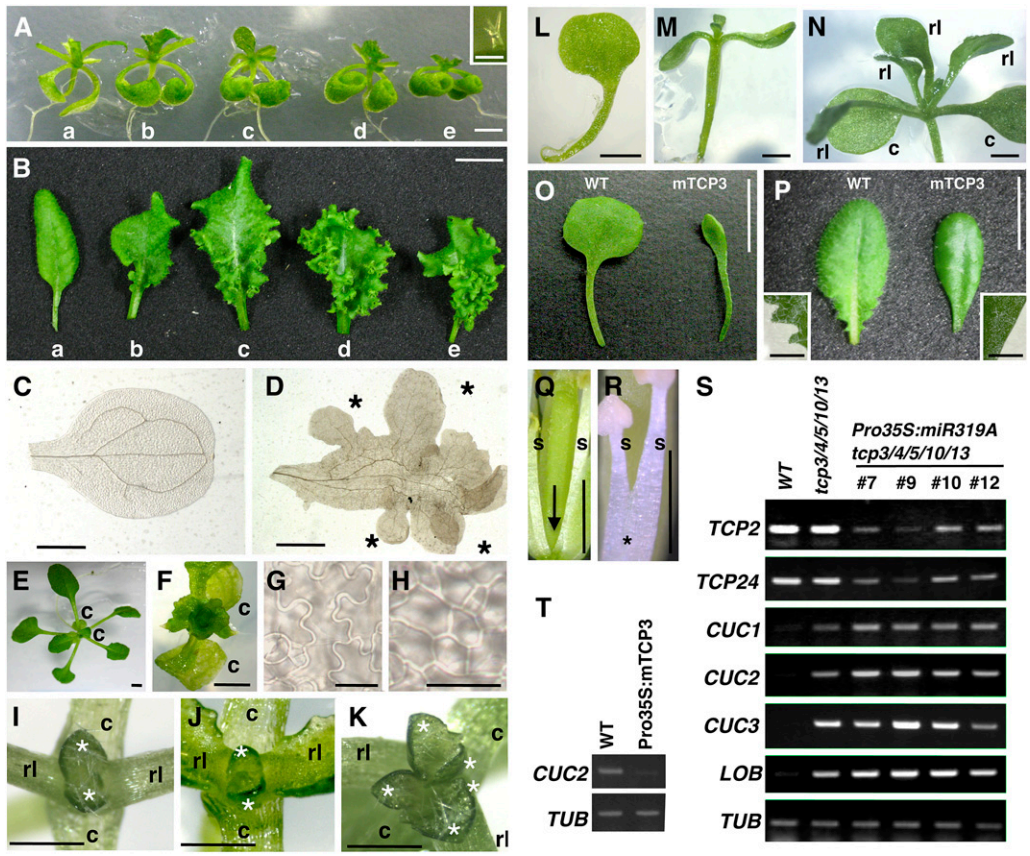

Figure 1. Dose-Dependent Effects of *CIN*-Like *TCP* Genes on Leaf Morphology and the Expression of Boundary-Specific Genes.

(A) and **(B)** Epinastic growth of cotyledons 14 d after germination **(A)** and wavy rosette leaves at the sixth position **(B)** in wild-type **(a)**, *tcp3/4/10* **(b)**, *tcp3/4/5/10* **(c)**, *tcp3/4/5/10/13* **(d)**, and *Pro35S:miR319A tcp3/4/5/10/13* **(e)**. Rosette leaves from the plants in **(A)** were detached for visualization in greater detail. Inset in **(A)** indicates the ectopic trichome on the cotyledons of *Pro35S:miR319A tcp3/4/5/10/13*.

(C) and **(D)** Vasculature of wild-type **(C)** and *Pro35S:miR319A tcp3/4/5/10/13* **(D)** cotyledons. The asterisks in **(D)** indicate the irregular vasculature at the tip and the margins.

(E) and **(F)** Three-week-old rosettes of wild-type **(E)** and *tcp3/4/5/10/13* **(F)** plants. The "c" indicates cotyledons.

(G) and **(H)** Epidermal cells of wild-type **(G)** and *tcp3/4/5/10/13* **(H)** leaves.

(I) through **(K)** Apical domains of wild-type **(I)**, *tcp3/4/5/10/13* **(J)**, and *Pro35S:miR319A tcp3/4/5/10/13* **(K)** seedlings. Asterisks indicate initiating rosette leaves. c, cotyledons; rl, rosette leaves (first and second).

(L) to **(N)** *Pro35S:mTCP3* plants with severe **(L)**, moderate **(M)**, and mild **(N)** phenotypes 14 d after germination. c, cotyledons; rl, rosette leaves.

(O) Rosette leaves of wild-type (WT; left) and the *Pro35S:mTCP3* plants with a moderate phenotype (right) at either the first or second position.

(P) Rosette leaves of wild-type (left) and the *Pro35S:mTCP3* plants with a mild phenotype (right) at the eighth position. The margins of the respective leaves are presented in the insets.

(Q) and **(R)** Stamens of wild-type **(Q)** and *Pro35S:mTCP3* plants with a mild phenotype **(R)**. s, stamens. Arrow in **(Q)** and asterisk in **(R)** indicate the separation and fusion of stamens, respectively.

(S) Expression of *TCP2*, *TCP24*, *CUC1*, *CUC2*, *CUC3*, and *LOB* in leaves at the fifth and sixth positions from wild-type, *tcp3/4/5/10/13*, and four independent lines of *Pro35S:miR319A tcp3/4/5/10/13* plants. Expression of the gene for tubulin (*TUB*) was monitored as an internal control.

(T) Expression of *CUC2* in leaves at the eighth, ninth, and tenth positions from the wild type and those from the *Pro35S:mTCP3* plants with a mild phenotype. PCR was terminated after 36 cycles. Expression of the gene for *TUB* was monitored as an internal control.

Bars = 1 mm in **(A)**, **(C)** to **(F)**, **(I)** to **(N)**, and the insets in **(P)** to **(R)**, 5 mm in **(B)**, **(O)**, and **(P)**, and 50 μm in the inset of **(A)**, **(G)**, and **(H)**.

(Figure 1P). Furthermore, *mir319a*^{129}, which contains a mutation in the *miR319A* locus and has a moderate increase of the expression of *TCP2*, *TCP3*, *TCP4*, *TCP10*, and *TCP24* (Nag et al., 2009), produced leaves with smooth margins (see Supplemental Figures 5A and 5B online). In addition, the stamens of these *Pro35S:mTCP3* plants were occasionally fused (Figures 1Q and 1R). These results were largely consistent with the previous report that the homozygous mutants of *LA* in tomato had fused cotyledons and lacked a functional SAM, whereas the heterozygous mutants had leaves with simple and lanceolate shapes (Mathan and Jenkins, 1962; Settler, 1964; Ori et al., 2007).

We reported that CIN-like TCPs act as negative regulators of expression of boundary-specific genes. Therefore, we examined the level of expression of these genes in our *tcp* mutants and *Pro35S:mTCP3* plants. In *tcp3/4/5/10/13* and *Pro35S:miR319A tcp3/4/5/10/13* plants, we detected the ectopic expression of boundary-specific genes, including *CUC1*, *CUC2*, *CUC3*, and *LATERAL ORGAN BOUNDARIES* (*LOB*) in the leaves (Figure 1S). By contrast, the level of expression of *CUC2*, which is involved in the formation of the serrations (Nikovics et al., 2006), was reduced in the leaves of *Pro35S:mTCP3* plants with a mild phenotype and in those of *mir319a*^{129} (Figure 1T; see Supplemental Figure 5C online). These results confirmed previous conclusions, derived from studies of *Pro35S:TCP3SRDX* plants, that *CIN*-like *TCP* genes regulate both the development of the SAM and leaves and the expression of boundary-specific genes (Koyama et al., 2007).

Genes Downstream of TCP3

Pro35S:TCP3SRDX induced a severely defective phenotype that hampered further efforts to identify the target genes of CIN-like TCPs. Therefore, we induced the transcription of *TCP3SRDX* using a LexA-VP16-estrogen receptor (XVE) system (*ProXVE:TCP3SRDX*). In this system, the expression of *TCP3SRDX* was induced by exogenous 17β-estradiol (estradiol; Zuo et al., 2000). We confirmed that *ProXVE:TCP3SRDX* plants exhibited severe defects in the expansion of their cotyledons when exposed to estradiol for 5 d after germination, whereas they had normal morphology when exposed to DMSO (see Supplemental Figures 6A and 6B online). The defective cotyledons of *ProXVE:TCP3SRDX* plants exposed to estradiol comprised rounded cells, which are the signature of the absence of differentiation (see Supplemental Figure 6B online). To identify the target genes of TCP3, a first set of microarray data was generated from *ProXVE:TCP3SRDX* plants exposed to DMSO or 5 μM estradiol for 24 h in liquid medium, although no visible morphological abnormalities were observed under these conditions. This microarray data and RT-PCR analysis revealed that the expression of boundary-specific genes, namely, *CUC1*, *CUC2*, *CUC3*, *LOB*, *LATERAL SUPPRESSOR*, and *CYP78A5/KLUH*, was induced in *ProXVE:TCP3SRDX* plants exposed to estradiol (see Supplemental Figure 7 and Supplemental Table 1 online). To eliminate potential indirect effects of the ectopic expression of *CUC* genes, we induced the expression of *TCP3SRDX* in *cuc1* and *cuc3* mutant seedlings because *TCP3SRDX* induced a dramatic increase of expression of *CUC1* and *CUC3* among boundary-specific genes (see Supplemental Table 1 online). In the *cuc1* and *cuc1 cuc3* backgrounds, the expression of *ProXVE:TCP3SRDX* had a reduced effect on the expansion of cotyledons compared with its effect in the wild-type background (see Supplemental Figures 6C through 6G online). Therefore, a second set of microarray data was generated from *ProXVE:TCP3SRDX cuc1* plants exposed to DMSO or 5 μM estradiol for 24 h in liquid medium.

The two sets of microarray experiments revealed that the expression levels of 1641 and 1675 genes were halved, with P values below 0.05 (false discovery rate [FDR] < 0.0122 and < 0.0287 in each experiment) in *ProXVE:TCP3SRDX* and *ProXVE:TCP3SRDX cuc1* plants, respectively, after exposure of seedlings to 5 μM estradiol for 24 h in liquid medium. The 1173 genes within the two data sets that overlapped were categorized as genes downstream of TCP3. We found many genes that contained binding motifs for TCP domains with significant probability in the region that extended 1000 bp upstream of each respective gene (see Supplemental Table 2 online). A GTGGnCCC motif is the binding sequence of the class II TCPs, which includes CIN-like TCPs, and a GGnCCC motif is the core binding sequence of both the class I and class II TCPs (Kosugi and Ohashi, 2002). Some variant sequences are presumed to be binding sites of TCPs (Martín-Trillo and Cubas, 2010). Our analyses suggested that those downstream genes could be directly regulated by TCP3.

Table 1. Changes in Expression of Genes Involved in Organ Morphogenesis Induced by *TCP3SRDX*

		ProXVE:TCP3SRDX		*ProXVE:TCP3SRDX cuc1*			
AGI Code[a]	Name	Change[b]	P Value	Change[b]	P Value	GGnCCC[c]	Reference
AT2G37630	*AS1*	0.264	0.0018	0.433	0.0051	+	Byrne et al. (2000)
AT4G01500	*NGA4*	0.329	0.0098	0.274	0.0008	+	Alvarez et al. (2009); Trigueros et al. (2009)
AT1G01030	*NGA3*	0.338	0.0001	0.354	0.0013	−	Alvarez et al. (2009); Trigueros et al. (2009)
AT1G14920	*GAI*	0.189	0.0027	0.267	0.0001	−	Hay et al. (2002)
AT5G41410	*BEL1*	0.412	0.0073	0.339	0.0004	−	Reiser et al. (1995)
AT5G03680	*PTL*	0.407	0.0026	0.408	0.0028	+	Brewer et al. (2004)
AT2G26580	*YAB5*	0.222	0.0017	0.323	0.0029	+	Izhaki and Bowman (2007)
AT4G36870	*SAW1*	0.444	0.0162	0.400	0.0010	−	Kumar et al. (2007)
AT3G17185	*TAS3*	0.449	0.0114	0.249	0.0009	+	Allen et al. (2005)
AT1G69440	*AGO7*	0.311	0.0176	0.299	0.0002	+	Hunter et al. (2003)
AT5G67440	*NPY3*	0.435	0.0035	0.450	0.0001	+	Cheng et al. (2008)

[a]AGI, Arabidopsis Genome Initiative.

[b]Changes are ratios from the plants exposed to DMSO (vehicle) to those exposed to estradiol. Average values were obtained from microarray experiments with three (*ProXVE:TCP3SRDX*) and four (*ProXVE:TCP3SRDX cuc1*) replicates.

[c]The GGnCCC motif is present (+) or absent (−) in the 1000-bp upstream region of the respective gene (http://www.arabidopsis.org/).

Comparative analysis demonstrated that the genes downstream of TCP3 overlapped, to a very considerable extent, a group of genes for auxin-inducible proteins, which included SMALL AUXIN UP RNA (SAUR) (Hagen and Guilfoyle, 2002), with the lowest P value of 3.403E-12 (as examined by Fischer's exact test) among 15,796 conserved domains, and an odds ratio of 8.33 (see Supplemental Table 3 online). Among *SAUR* genes that have highly similar nucleotide sequences, rice (*Oryza sativa*) *SAUR39* was shown to act as a negative regulator for auxin synthesis and transport (Kant et al., 2009). We then used *At1g29460* and *At5g18020*, which were similar and different isoforms of rice *SAUR39*, respectively, for further analysis. In addition, the genes downstream of TCP3 also overlapped six of 29 members of the *AUX/IAA* family, which repress transcription of auxin-inducible genes (see Supplemental Table 4 online; Liscum and Reed, 2002). Interestingly, the expressions of six of seven genes for the PIN-FORMED (PIN) family of auxin efflux carriers were significantly changed by *TCP3SRDX* (see Supplemental Table 5 online; Benková et al., 2003). *PIN1*, *PIN5*, and *PIN6* were upregulated by *TCP3SRDX*, whereas *PIN3*, *PIN4*, and *PIN7* were downregulated. These observations suggested that TCP3 might be involved in regulation of the response to auxin.

Known regulators of leaf development were identified as putative targets of TCP3 (Table 1; see Supplemental Table 6 online). These included *AS1*, *PETAL LOSS* (*PTL*), *YABBY5*, *SAW1*, *GA INSENSITIVE* (*GAI*), *ARGONAUTE7* (*AGO7*)/*ZIPPY*, and trans-*Acting siRNA3* (*TAS3*) (Byrne et al., 2000; Hay et al., 2002; Hunter et al., 2003; Garcia et al., 2006; Izhaki and Bowman, 2007; Kumar et al., 2007). Resembling *CIN*-like *TCP* genes, loss of the *NGATHA* (*NGA*) genes results in exaggerated serration of leaves, whereas the ectopic expression of *NGA* genes induces the fusion of cotyledons (Alvarez et al., 2009; Trigueros et al., 2009). Among these genes, we focused on *AS1* as a downstream gene of TCP3 because the abnormal phenotype of the *as1* leaves is enhanced by mutations in *AGO7/ZIPPY*, *SAW1*, and *GAI* (Hay et al., 2002; Garcia et al., 2006; Kumar et al., 2007).

We examined the levels of expression of the genes downstream of TCP3 in several genetic backgrounds and experimental conditions. RT-PCR analysis revealed that the levels of expression of *AS1*, *IAA3/SHY2*, *IAA4*, and two *SAUR* genes, *At1g29460* and *At5g18020*, were reduced in wild-type and *cuc* mutant backgrounds (*ProXVE:TCP3SRDX*, *ProXVE:TCP3SRDX cuc1*, and *ProXVE:TCP3SRDX cuc1 cuc3*) upon induction of *TCP3SRDX* for 24 h (Figure 2A). The reduced levels of expression of these target genes were observed over a short interval of 8 h after the start of induction of *TCP3SRDX* (see Supplemental Figure 8 online). In addition, the expression levels of *AS1*, *IAA3/SHY2*, and *At1g29460* were reduced in *Pro35S:miR319A tcp3/4/5/10/13* plants (Figure 2B). These observations suggested that TCP3 might activate the expression of *AS1*, *IAA3/SHY2*, and *At1g29460*.

In addition, ontological analysis of the genes downstream of TCP3 revealed enrichment for genes encoding proteins found in chloroplasts or plastids (see Supplemental Figure 9 online). This group included the *LIPOXYGENASE2* gene, whose product regulates biosynthesis of jasmonate and is downregulated in *jaw-d* mutants (Schommer et al., 2008). Furthermore, we also found genes for known regulators of developmental timing (see Supplemental Table 7 online), which appeared to cause the delayed flowering in *tcp3/4/5/10/13* mutants or ectopic trichomes in *Pro35S:miR319A tcp3/4/5/10/13* plants (Figure 1A; see Supplemental Figure 3 online).

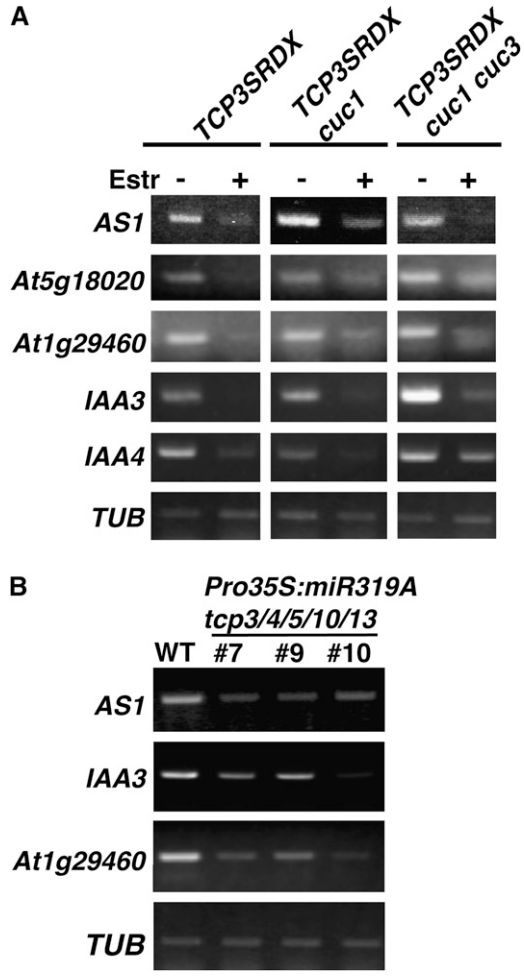

Figure 2. Expression of Genes Downstream of TCP3.

(A) RT-PCR analysis of expression of genes downstream of TCP3 after induction or noninduction of *TCP3SRDX* in wild-type (WT) and *cuc* mutant backgrounds. Samples of RNA were prepared from whole plants that had been maintained in liquid medium supplemented with DMSO (−) or estradiol (Estr; +) for 24 h. Expression of the *TUB* gene was monitored as an internal control.

(B) RT-PCR analysis of expression of genes downstream of TCP3 in three independent lines of *Pro35S:miR319A tcp3/4/5/10/13* plants. RNA was prepared from whole 7-d-old seedlings grown on the plate. Expression of the *TUB* gene was monitored as an internal control.

AS1, *miR164A*, *IAA3/SHY2*, and *At1g29460* Are the Direct Targets of TCP3

We examined the direct binding of TCP3 to the promoters of the downstream genes by chromatin immunoprecipitation (ChIP) with TCP3-specific antibodies (see Supplemental Figure 10 online). In addition to *AS1*, *IAA3/SHY2*, and *At1g29460*, we included a

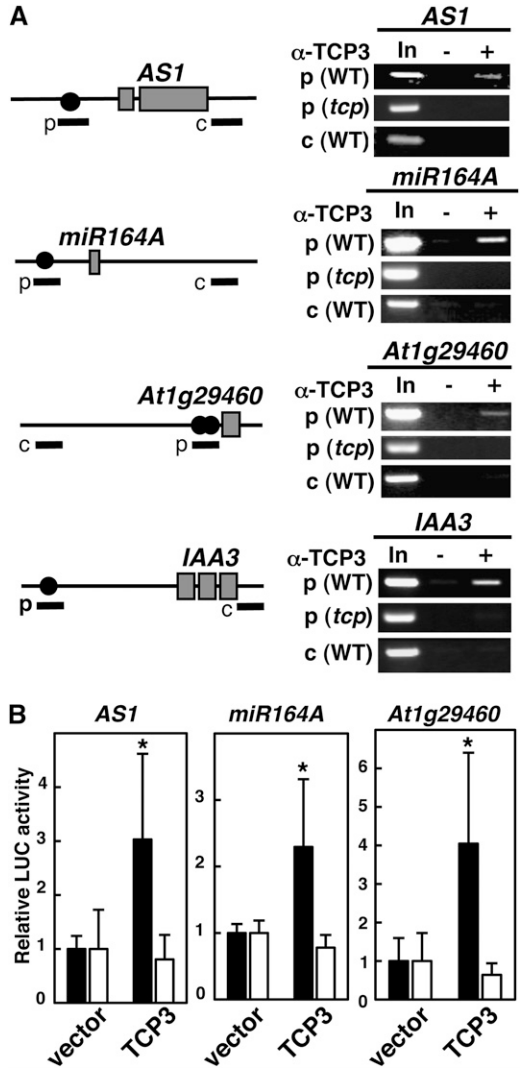

Figure 3. ChIP and Transient Gene Expression Analyses of the Direct Binding of TCP3 to the Promoters of Target Genes.

(A) ChIP analysis. The left side of panel **(A)** shows relevant regions of the *AS1*, *miR164A*, *At1g29460*, and *IAA3/SHY2* genes. Black circles and gray boxes indicate GGnCCC motifs and exons, respectively. The position of the GGnCCC motif relative to the putative site of transcription initiation is as follows. *AS1*, −955 bp; *miR164A*, −976 bp; *At1g29460*, −120 and −258 bp; and *IAA3*, −2011 bp. Thick black bars below genes indicate the regions amplified by PCR and correspond to each promoter (p) and control (c) in the right panel. The right panel shows the enrichment for the relevant PCR-amplified fragments in the chromatin from wild-type (WT) and *tcp3/4/10* (*tcp*) plants, respectively, precipitated by TCP3-specific antibodies (α-TCP3). "In" indicates the input control. ChIP reaction mixtures were processed in the absence (−) and presence (+) of antibodies.

(B) Transient gene expression analysis of the *TCP3* effector plasmid. *LUC* activities obtained after cobombardment of the control effector and with the each reporter plasmid are set at 1. Black and white bars represent the relative activities of *LUC* driven by wild-type and mutated promoters of *AS1*, *miR164A*, and *At1g29460*, respectively. The mutated promoter of *At1g29460* contained nucleotide replacements in both GGnCCC motifs. Error bars indicate SD ($n = 3$). Asterisks indicate the significant difference from the values of the control by Student's t test ($P < 0.05$).

precursor gene for miR164, which is a possible downstream gene of TCP3 (Koyama et al., 2007), in the ChIP analysis. Although our microarray did not have spots corresponding to three precursor genes for miR164, the *miR164A* gene contains a GGnCCC motif in its 5′ upstream region, and this gene makes the largest contribution to the accumulation of miR164 in leaves (Nikovics et al., 2006; Sieber et al., 2007). Therefore, we included *miR164A* in our analysis. ChIP analysis using chromatin from wild-type plants revealed clear enrichment for the respective fragments, generated by PCR, that correspond to the regions containing the GGnCCC motif in the promoters, but not control regions, of *AS1*, *miR164A*, *IAA3/SHY2*, and *At1g29460* (Figure 3A). For the negative control, ChIP analysis using the chromatin from *tcp3/4/10* plants detected no enrichment for the fragments corresponding to these promoters (Figure 3A). These results indicated that TCP3 binds directly to the promoters of *AS1*, *miR164A*, *IAA3/SHY2*, and *At1g29460.*

To confirm the binding of TCP3 to the GGnCCC motif of the promoters of *AS1, miR164A,* and *At1g29460* in plant cells, we performed transient expression assays using a reporter gene driven by the promoters of *AS1*, *miR164A*, and *At1g29460*, respectively. The TCP3 effector activated the expression of each reporter-gene construct but not that of the reporter gene when it was driven by a promoter with a mutated GGnCCC motif (Figure 3B). These results confirmed that TCP3 activated the expression of *AS1*, *miR164A*, and *At1g29460* via direct binding to the GGnCCC motif in each respective promoter.

Regulation of the Promoter Activities of *AS1*, *miR164A*, *IAA3/SHY2*, and *At1g29460* by TCP3

We examined the effects of TCP3SRDX on the spatial regulation of the promoter activities of *AS1*, *miR164A*, *IAA3/SHY2*, and *At1g29460* in cotyledons and young leaves, using a β-*glucuronidase* (*GUS*) reporter gene driven by the promoter of each gene. The promoter activity of *AS1*, as visualized by blue staining of GUS activity, was observed in cotyledons and leaves (Figure 4A; Iwakawa et al., 2007). The pattern of activity of *ProAS1:GUS* was similar to that of *ProTCP3:GUS* (Koyama et al., 2007). By contrast, the activity of *ProAS1:GUS* was markedly reduced in cotyledons of *ProAS1:GUS Pro35S:TCP3SRDX* plants (Figure 4B), indicating that TCP3SRDX interfered with the activity of the *AS1* promoter. The reduced activity of *ProAS1:GUS* might be caused by both the direct and indirect effects of TCP3SRDX, since severe developmental defects were present in *ProAS1:GUS Pro35S:TCP3SRDX* plants.

In wild-type plants, the promoter activity of *miR164A* was detected specifically in the basal regions, marginal regions, veins, and tips of developing leaves, as reported previously (Figure 4C; Nikovics et al., 2006). By contrast, in *PromiR164A:GUS Pro35S:TCP3SRDX* plants, the promoter activity of *miR164A* was not observed in these organs and tissues, except in the cotyledonary tips (Figure 4D). Our results suggested that the reduced accumulation of miR164 in *Pro35S:TCP3SRDX* plants (Koyama et al., 2007) was due to the direct repression of the *miR164A* promoter activity.

The promoters of the *IAA3/SHY2* (Tian et al., 2002) and *At1g29460* genes were very active both in cotyledons and in

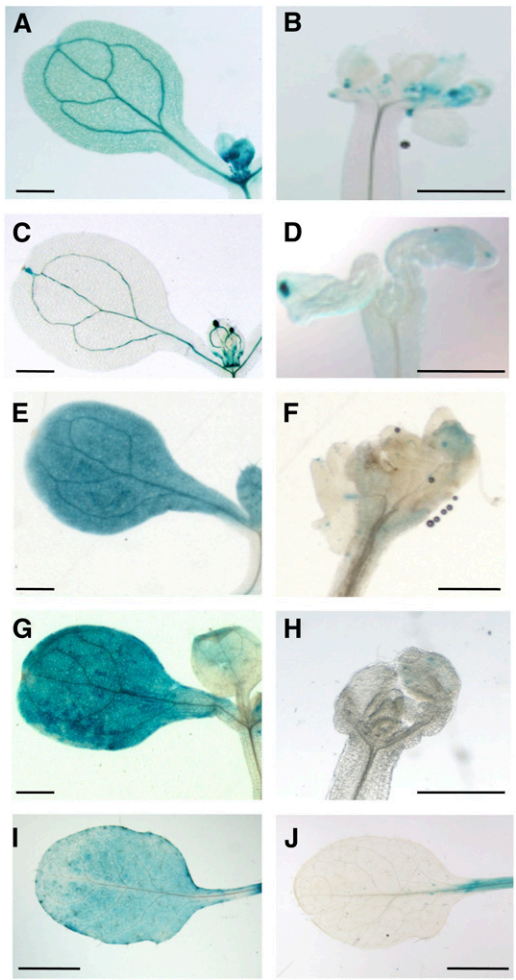

Figure 4. Effects of Chimeric TCP3 Repressors on the Spatial Expression of Target Genes.

(A) to **(H)** GUS reporter activity (blue color) driven by the promoters of *AS1* (**[A]** and **[B]**), *miR164A* (**[C]** and **[D]**), *IAA3/SHY2* (**[E]** and **[F]**), and *At1g29460* (**[G]** and **[H]**) in wild-type (**[A]**, **[C]**, **[E]**, and, **[G]**) and *Pro35S:TCP3SRDX* (**[B]**, **[D]**, **[F]**, and **[H]**) plants.
(I) and **(J)** Activities due to *ProAt1g29460:GUS* **(I)** and *PromAt1g29460:GUS* **(J)** in rosette leaves.
Bars = 0.5 mm in **(A)** to **(H)** and 5 mm in **(I)** and **(J)**.

leaves, but these activities were dramatically reduced upon coexpression of *TCP3SRDX* (Figures 4E to 4H). In addition, mutation of the two GGnCCC motifs in the promoter of *At1g29460* (*PromAt1g29460:GUS*) decreased its activity considerably (Figures 4I and 4J). These results suggested that TCP3 activated *At1g29460* via interaction with the GGnCCC motifs in intact plants.

The Negative Effects of TCP3 on the Auxin Response

Since IAA3/SHY2 has been shown to suppress the auxin response (Hamann et al., 2002; Tian et al., 2002; Dello Ioio et al., 2008), and a rice *SAUR* gene has been shown to act as a negative regulator of the accumulation and transport of auxin (Kant et al., 2009), it is likely that TCP3SRDX derepresses the auxin response. To analyze the effects of TCP3SRDX on the auxin response, we investigated the expression of a *GUS* reporter gene driven by the *DR5* promoter (*ProDR5:GUS*; Ulmasov et al., 1997) in *ProXVE:TCP3SRDX* plants. The GUS activity in *ProDR5:GUS ProXVE:TCP3SRDX* plants under noninducing conditions (exposure to DMSO) was observed at the tips of developing leaves, as reported previously (Figure 5A; Benková et al., 2003). When 5 μM estradiol was provided to seedlings for 4 d after germination, the promoter activity of *DR5* was observed in the tips of outgrowths, at the margins, and in the epinastic blades of cotyledons (Figure 5B).

We further examined the expression of auxin-inducible genes in *ProXVE:TCP3SRDX* plants. The ectopic *GUS* activity of *ProDR5:GUS ProXVE:TCP3SRDX* plants required the exposure to 5 μM estradiol for 48 h in liquid medium (see Supplemental Figures 11A and 11B online). Consistent with this, the basal levels of expression of *LBD16* (Okushima et al., 2007) and *At4g12410* (*SAUR*), nondirect targets of TCP3, were increased by exposure to estradiol for 48 h, but not for 24 h, in liquid medium (see Supplemental Figures 11C and 11D online). Interestingly, the auxin-inducible expression of *LBD16* was magnified by continuous expression of *TCP3SRDX* for 48 h, whereas that of *At4g12410* was unaffected by *TCP3SRDX* (see Supplemental Figure 11D online). By contrast, the expression of *IAA3/SHY2*, *IAA4*, *At1g29460*, and *At5g18020* was downregulated in *ProXVE:TCP3SRDX* plants after exposure to 5 μM estradiol for 24 and 48 h (see Supplemental Figures 11C and 11D online). The levels of expression of these genes were partially restored but remained lower than those of the control by exposure of the plants to exogenous auxin for 1 h (see Supplemental Figures 11C and 11D online). These results suggested that *TCP3SRDX* derepressed the expression of several auxin-inducible genes.

To analyze further the negative effects of TCP3 on the auxin response, we examined the sensitivity of *Pro35S:mTCP3* plants with moderate increases in the expression of *IAA3/SHY2*, *IAA4*, *At1g29460*, and *At5g18020* to exogenous auxin (Figures 5C to 5E; see Supplemental Figure 12 online). Although exogenous auxin induced epinastic growth of wild-type cotyledons, it did not change the direction of growth of the *Pro35S:mTCP3* cotyledons (Figures 5C to 5H). All 65 wild-type seedlings tested showed epinastic growth, whereas 54 out of 70 *Pro35S:mTCP3-1* seedlings and 64 out of 80 *Pro35S:mTCP3-13* seedlings did not show epinastic growth. The morphology of the *Pro35S:mTCP3* cotyledons contrasted with the epinastic cotyledons of the various *tcp* mutants under normal conditions (Figure 1A).

The negative effect of *TCP3* on the auxin response was also observed with respect to the regulation of cellular differentiation in *Pro35S:mTCP3* and *tcp3/4/5/10/13* plants. Exogenous auxin induced dedifferentiation of cells in the hypocotyl of 48 out of 53 wild-type seedlings, but not in the cotyledons, under our experimental conditions (Figure 5I). By contrast, exogenous auxin did not induce dedifferentiation of cells in *Pro35S:mTCP3* hypocotyls (Figure 5J). Normal morphology was observed in the cotyledons of 29 out of 50 *Pro35S:mTCP3-1* seedlings and 30 out of 46 *Pro35S:mTCP3-13* seedlings. Moreover, exogenous auxin accelerated dedifferentiation in the hypocotyl and cotyledons of *tcp3/4/5/10/13* plants (Figure 5K). All 73 *tcp3/4/5/10/13*

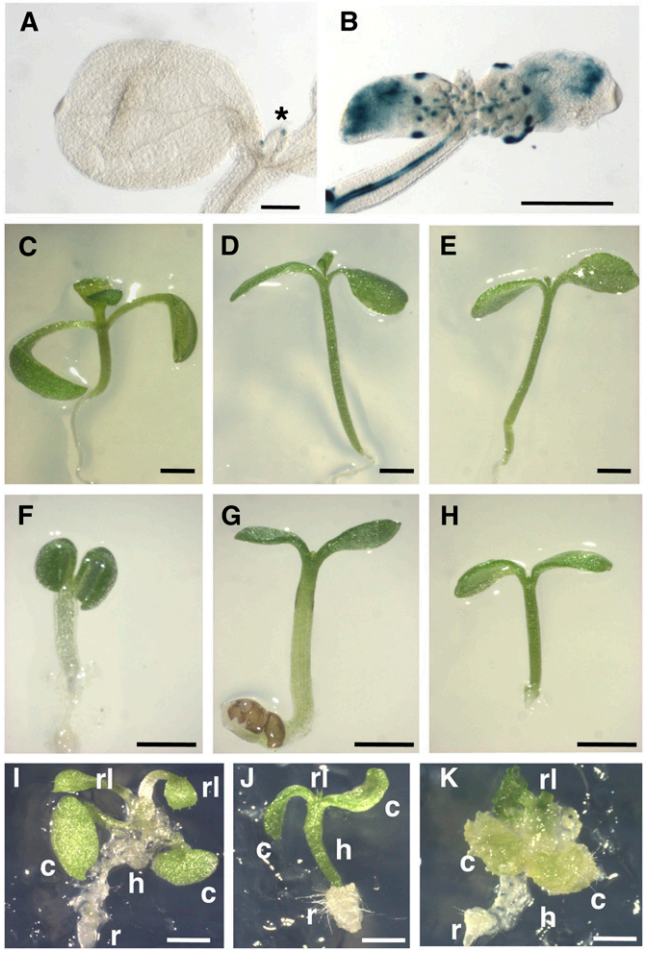

Figure 5. The Negative Effect of TCP3 on the Auxin Response.

(A) and **(B)** GUS activity driven by the *DR5* promoter after noninduction **(A)** and induction **(B)** of *TCP3SRDX*. The asterisk in **(A)** indicates the signal due to *GUS* at the tip of developing leaves.
(C) to **(H)** Wild-type (**[C]** and **[F]**) and two independent lines of *Pro35S:mTCP3* (**[D]**, **[E]**, **[G]**, and **[H]**) seedlings grown on plates containing DMSO (**[C]** to **[E]**) or on plates containing 10 μM naphthalene acetic acid (**[F]** to **[H]**) for 7 d.
(I) through **(K)** Cellular differentiation of wild-type **(I)**, *Pro35S:mTCP3* **(J)**, and *tcp3/4/5/10/13* **(K)** seedlings grown on plates containing 10 μM naphthalene acetic acid for 15 d. c, cotyledon; h, hypocotyl; r, root; rl, rosette leaf.
Bars = 0.5 mm.

seedlings tested showed cellular dedifferentiation in their hypocotyls, and 33 of them showed cellular dedifferentiation in their cotyledons. These results suggested that *TCP3* had a negative effect on the auxin response.

Regulation of *CUC* Genes by the Products of Genes That Are Direct Targets of TCP3

We examined the involvement of the direct target genes of TCP3, namely *AS1*, *miR164A*, *IAA3/SHY2*, and *At1g29460*, in the regulation of *CUC* genes. The posttranscriptional negative effect of *miR164A* on the expression of *CUC1* and *CUC2* has been clearly demonstrated (Nikovics et al., 2006; Sieber et al., 2007); however, the involvement of *AS1*, *IAA3/SHY2*, and *At1g29460* in regulating the expression of *CUC* genes remains to be characterized. The ectopic expression of the *AS1*, *miR164A*, *IAA3/SHY2*, and *At1g29460* genes, respectively, induced fused cotyledons and the absence of functional SAMs in *cuc1* and *cuc3* mutant backgrounds, as also observed in *Pro35S:mTCP3* plants and in the *cuc1 cuc3* double mutant (Hibara et al., 2006; Koyama et al., 2007). The ectopic expression of these genes in a wild-type background induced only slight phenotypic abnormalities (Table 2, Figures 6A to 6J). In the *cuc3* background, the expression levels of *CUC1* and *CUC2* were reduced by ectopic expression of *AS1*, *miR164A*, *IAA3/SHY2*, or *At1g29460* (Figure 6K). These results suggested that the products of *AS1*, *miR164A*, *IAA3/SHY2*, and *At1g29460* might partially but cooperatively repress the expression of *CUC* genes.

The cooperative functions of *AS1* and *miR164A* as negative regulators of the expression of *CUC* genes were also evident from their synergistic effects on the morphogenesis of leaves. The *as1* and *mir164a* single mutants had crinkled and serrated leaves, whereas leaves of *as1 mir164a* double mutant plants had remarkably deep sinuses at their margins (Figure 7A). These abnormalities were an indication of the cooperative functions of the products of *AS1* and *miR164A* in leaf morphogenesis. In parallel with these morphological changes, we observed the

Table 2. Phenotypic Changes Induced by Ectopic Expression of Target Genes of TCP3

	Classification of Phenotype (%)		
Genotype (*n*)[a]	Heart-Shaped[b]	*stm*-Like[c]	Cup-Shaped[d]
Pro35S:AS1 (250)	0.80	0.40	0.00
Pro35S:AS1/cuc1 (135)	8.89	4.44	5.20
Pro35S:AS1/cuc3 (206)	8.25	0.97	0.97
Pro35S:miR164A (209)	10.50	1.43	0.48
Pro35S:miR164A/cuc1 (100)	40.00	10.0	8.00
Pro35S:miR164A/cuc3 (141)	61.70	2.83	22.70
Pro35S:IAA3 (293)	0.68	0.34	0.00
Pro35S:IAA3/cuc1 (121)	6.61	0.83	0.00
Pro35S:IAA3/cuc3 (266)	8.27	1.13	0.75
Pro35S:At1g29460 (299)	1.00	1.00	0.00
Pro35S:At1g29460/cuc1 (179)	4.48	2.79	0.00
Pro35S:At1g29460/cuc3 (213)	6.57	1.41	0.00
Pro35S vector/cuc1 (174)	1.72	0.00	0.00
Pro35S vector/cuc3 (172)	1.74	0.00	0.00

The numbers do not add up to 100% since the rest of plants had normal morphology.
[a]Number of plants examined.
[b]One side of each cotyledon was fused to the other cotyledon. SAM activity was occasionally defective.
[c]SAM activity was defective, but cotyledons were fused only at the base or not fused.
[d]Both sides of each cotyledon were fused, and the SAM was defective.

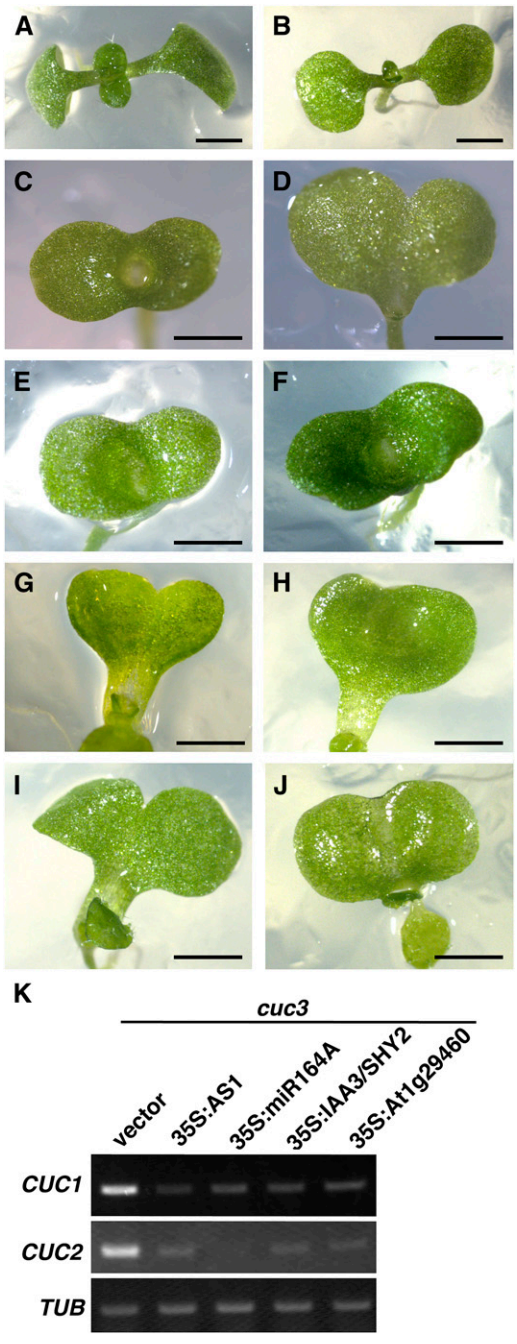

Figure 6. Fusion of Cotyledons Induced by Ectopic Expression of *AS1*, *miR164A*, *IAA3/SHY2*, and *At1g29460* in the *cuc1* and *cuc3* Backgrounds.

(A) to **(J)** Transgenic seedlings of the T1 generation after transformation with the vector control (**[A]** and **[B]**), *Pro35S:AS1* (**[C]** and **[D]**), *Pro35S:miR164A* (**[E]** and **[F]**), *Pro35S:IAA3/SHY2* (**[G]** and **[H]**), and *Pro35S:At1g29460* (**[I]** and **[J]**) in the *cuc1* (**[A]**, **[C]**, **[E]**, **[G]**, and **[I]**) and the *cuc3* (**[B]**, **[D]**, **[F]**, **[H]**, and **[J]**) backgrounds. Bars = 1 mm

(K) Expression of *CUC1* and *CUC2* in 7-d-old *cuc3* seedlings after transformation with the specified constructs. The RNA samples were harvested from normal seedlings transformed with the vector or heart-shaped seedlings transformed with the respective constructs of *Pro35S:AS1*, *Pro35S:miR164A*, *Pro35S:IAA3/SHY2*, and *Pro35S:At1g29460*. Expression of the *TUB* gene was monitored as an internal control.

[See online article for color version of this figure.]

additive effects of these gene products on the regulation of the *CUC* genes in the *as1 mir164a* mutant. In *as1 mir164a* double mutants, we detected the ectopic expression of *CUC1*, *CUC2*, and *CUC3* in leaves, whereas the *as1* and *mir164* single mutants ectopically expressed *CUC3* and *CUC1* plus *CUC2*, respectively (Figure 7B; Nikovics et al., 2006; Sieber et al., 2007). The cooperative regulation of the expression of *CUC* genes appeared to induce morphological changes at the leaf margins and raised the level of expression of the *KNAT1* gene (Figure 7B). These results are consistent with reports of an antagonistic pathway involving *AS1* and *CUC* genes that leads to the formation of the SAM and the development of floral organs (Hibara et al., 2003; Xu et al., 2008). By contrast, *as1* did not affect the level of expression of *TCP3* (Figure 7C), indicating that the expression of *TCP3* is not controlled by AS1.

DISCUSSION

The Molecular Basis of the Regulatory Network Dominated by CIN-Like TCPs

In this study, we analyzed the regulatory network that is dominated by CIN-like TCPs during the differentiation of leaves. We demonstrated that TCP3 suppresses the expression of *CUC* genes via direct activation of the expression of *miR164A*, *AS1*, *IAA3/SHY2*, and *At1g29460* (Figure 8A). Phenotypic analysis of plants with multiple mutations in *CIN*-like *TCP* genes indicated that CIN-like TCPs act redundantly to regulate similar sets of genes. Our observations that the products of *AS1*, *miR164A*, *IAA3/SHY2*, and *At1g29460* acted negatively and differentially to regulate the expression of individual *CUC* genes revealed that these direct target genes of TCP3 partially but cooperatively repress the expression of *CUC* genes. The genetically redundant and differentially regulated pathways are related to the negative interaction between *CIN*-like *TCP* genes and *CUC* genes. In this study, we expanded on extensive prior studies on the functions of CIN-like TCPs (Nath et al., 2003; Palatnik et al., 2003; Koyama et al., 2007; Ori et al., 2007; Efroni et al., 2008; Schommer et al., 2008). We demonstrate the molecular basis of the regulatory network comprising *AS1*, miR164, and repressors of the auxin response, which promotes the differentiation of leaves.

The negative regulation of *CUC* genes by CIN-like TCPs is the core process in the coordination of the promotion of differentiation of leaf cells and the elimination of the undifferentiated fate of cells in leaves. *CUC* genes positively regulate the activity of *KNOX* genes (Aida et al., 1999; Hibara et al., 2003), which promote the undifferentiated fate of cells. By contrast, CIN-like TCPs negatively regulate the expression of *CUC* genes to inhibit the undifferentiated fate. The expression of *CUC* genes is differentially regulated at both the transcriptional and the posttranscriptional levels. miR164 negatively regulates the expression of *CUC1* and *CUC2* posttranscriptionally, whereas AS1 regulates the transcription of *CUC3* (Sieber et al., 2007; this study). Auxin

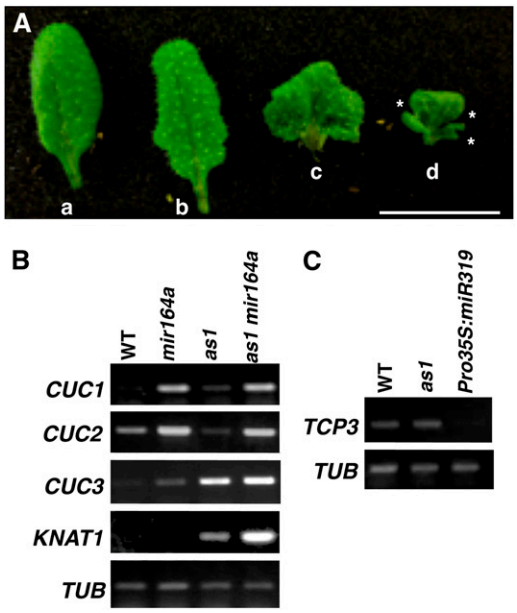

Figure 7. Cooperative Functions of *AS1* and *miR164A* in Leaf Morphogenesis and the Negative Regulation of Boundary-Specific Genes.

(A) Leaves of wild-type **(a)**, *mir164a* **(b)**, *as1* **(c)**, and *as1 mir164a* **(d)** plants. Asterisks indicate the deep sinuses in the *as1 mir164a* leaf. Bar = 1 cm.

(B) RT-PCR analysis of *CUC* and *KNOX* gene expression. Samples of RNA were prepared from rosette leaves of the plants indicated. Expression of the *TUB* gene was monitored as an internal control. WT, wild type.

(C) RT-PCR analysis of *TCP3* gene expression. Samples of RNA were prepared from rosette leaves of the plants indicated. *Pro35S:miR319* plants were used as negative controls for the expression of *TCP3*. Expression of the *TUB* gene was monitored as an internal control.

[See online article for color version of this figure.]

appears to define the spatial expression of *CUC* genes (Furutani et al., 2004; Heisler et al., 2005; this study). These diverse modes of regulation appear to be important in specifying both the timing and the localization of the expression of *CUC* genes. Moreover, consistent with the *CUC*-dependent regulation of *KNOX* genes, *AS1* and auxin negatively regulate the activity of *KNOX* genes (Byrne et al., 2000; Hay et al., 2006; Guo et al., 2008). Thus, CIN-like TCPs probably suppress the activity of *KNOX* genes to promote the differentiated fate through both *CUC*-dependent and *CUC*-independent pathways.

Considering our observations that CIN-like TCPs directly activate key developmental regulators, namely, AS1, miR164, and the auxin response, we postulated that CIN-like TCPs are located in the upstream region of the regulatory network that controls the differentiation of leaves. Several modules downstream of CIN-like TCPs can be delineated. In the first module, *AS1* is a functional node that promotes differentiation of leaves. CIN-like TCPs activate the expression of *AGO7*/*ZIPPY*, *SAW1*, and *GAI*, which cooperate with *AS1* in the differentiation of leaves (Hay et al., 2002; Garcia et al., 2006; Kumar et al., 2007). With respect to the antagonistic interactions between *AS1* and *KNOX* genes, and the inhibitory regulation of *KNOX* genes by CIN-like TCPs (Byrne et al., 2000; Koyama et al., 2007; Ori et al., 2007), we propose that CIN-like TCPs maintain the activity of AS1 in both direct and indirect manners. In the second module, CIN-like TCPs play a critical role in the accumulation of miR164, which negatively regulates the expression of *CUC1* and *CUC2* in leaves, by direct activation of *miR164A*, which encodes the main isoform of miR164 that functions in leaves (Nikovics et al., 2006; Sieber et al., 2007). miR164 prevents fluctuations in the expression of its target genes (Sieber et al., 2007). Therefore, CIN-like TCPs might increase the stability of developmental programs. In the third module, CIN-like TCPs regulate morphology by activating the expression of genes that encode repressors of the

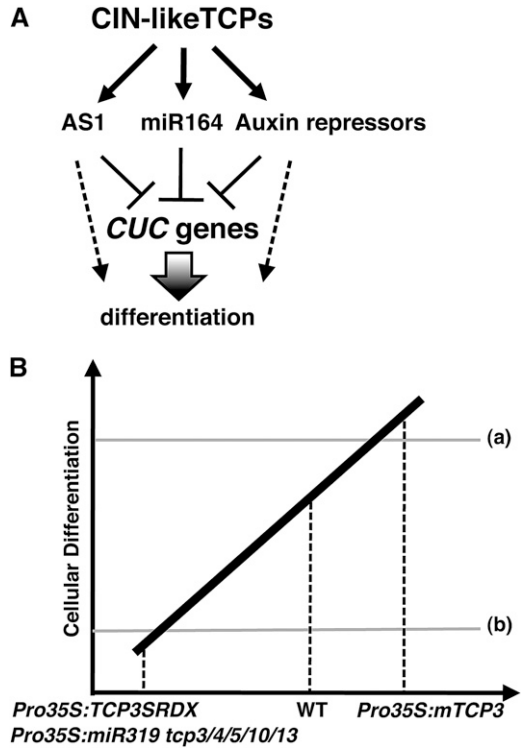

Figure 8. The Putative Roles of *CIN*-Like *TCP* Genes.

(A) The regulatory network in which CIN-like TCPs negatively, and indirectly, regulate the expression of *CUC* genes. CIN-like TCPs are upstream regulators that promote the differentiated fate in leaves. The regulatory network consists of three modules, which involve the activities of AS1, miR164, and auxin repressors, respectively. Each module partially, but cooperatively, represses the expression of *CUC* genes. Dashed lines indicate *CUC*-independent pathways that possibly promote the differentiated fate.

(B) *CIN*-like *TCP* genes act dose dependently as master regulators of leaf development. TCP activity above the threshold indicated by (a) inhibits the formation of the SAM. TCP activity below the threshold indicated by (b) facilitates formation of shoot meristems. The difference between (a) and (b) is large enough to allow generation of a variety of leaf forms. TCP activity corresponding to the wild type (WT) generates flat and simple leaves. Higher TCP activity than that of the wild type (as in *Pro35S:mTCP3*) generates *la*-like leaves, whereas lower activity (as in *Pro35S:TCP3SRDX* and *Pro35S:miR319 tcp3/4/5/10/13*) promotes wavy leaf surfaces and margins.

auxin response. CIN-like TCPs are likely to maintain the sensitivity of leaf cells to auxin responses of various magnitudes within a very narrow range. IAA3/SHY2 inactivates AUXIN RESPONSE FACTOR7 (ARF7) and ARF19 via a physical interaction. Therefore, TCP3SRDX might suppress expression of *IAA3*/*SHY2*, which in turn activates these ARFs and derepresses the expression of their targets, such as *LBD16* (Weijers et al., 2005; Okushima et al., 2007). In addition, we showed that TCP3SRDX reduced the expression levels of *TAS3* and *AGO7*/*ZIPPY*, which are involved in the posttranscriptional negative regulation of *ARF2*, *ARF3*, and *ARF4* (Table 1; Adenot et al., 2006; Fahlgren et al., 2006; Garcia et al., 2006; Hunter et al., 2006). The deregulation of *ARF3* by *TAS3* induces deeply serrated leaves (Fahlgren et al., 2006), suggesting important roles of *TAS3* and *AGO7*/*ZIPPY* downstream of CIN-like TCPs. Precise responses to auxin have been shown to determine the final size and shape of leaves, the pattern of the vasculature, the directions of cotyledonary growth, and the fate of cellular differentiation (Hu et al. 2003; Cheng et al., 2006; Scarpella et al., 2006; Hay et al., 2006). We propose that the auxin responses integrate the regulation of *CUC* genes and other processes of the differentiation of leaves downstream of *CIN*-like *TCP*s.

We demonstrated the contribution of *CIN*-like *TCP* genes to the development of both the SAM and leaves, using plants with multiple mutations in *CIN*-like *TCP* genes, and our results were consistent with our previous findings obtained using the chimeric TCP repressors (Koyama et al., 2007). Our model for the actions of *CIN*-like *TCP* genes is shown in Figure 8B. The activity of CIN-like TCPs corresponding to the wild type results in flat and simple leaves. Decrease in this activity results in serration, wavy surfaces, and delayed differentiation of leaves. Further reduction in the activities of the products of *CIN*-like *TCP* genes, as observed in *Pro35S:miR319A tcp3/4/5/10/13* and *Pro35S:TCP3SRDX* plants with severely abnormal phenotypes, induces the acquisition of meristematic fates in leaves and the expansion of the region in which shoots are formed. On the other hand, increase in the activity of CIN-like TCPs, as observed in *mir319a*^{129} and *Pro35S:mTCP3* plants with mild and moderate phenotypes, results in leaves with smooth margins and a *la*-like form due to precocious differentiation. Further increase in the activity of TCP3, as observed in *Pro35S:mTCP3* plants with a severe phenotype, induces a lack of a functional SAM (Koyama et al., 2007). Therefore, the graduated regulation of the differentiated fate by CIN-like TCPs, as well as regulatory modules downstream of these TCPs, has an important role in specifying a broad range of signals for leaf development without any disruptive effects on plant growth.

A Possible Role for *CIN*-Like *TCP* Genes in Generating Different Leaf Forms

Knockout of *CIN*-like *TCP* genes induced the formation of serrated and wavy leaves, and the extent of each morphological abnormality was correlated with the number of TCP genes that we disrupted. Thus, the possibility exists that CIN-like TCPs might have exerted an evolutionary role in the development of leaves of different shapes and characteristics. In compound leaves, the timing of differentiation is delayed compared with that for simple leaves (Hareven et al., 1996; Champagne and Sinha, 2004; Hay and Tsiantis, 2006). *KNOX* genes are required for the dissection that results in the formation of compound leaves, and ectopic expression of KNOX genes increases such dissection (Hareven et al., 1996; Hay and Tsiantis, 2006). This KNOX-mediated regulation of the nature of leaf margins requires auxin and the activities of the products of *CUC* genes (Barkoulas et al., 2008; Blein et al., 2008; Berger et al., 2009; Koenig et al., 2009). Given that CIN-like TCPs negatively regulate some aspects of the auxin response and the expression of *CUC* genes, we postulate that CIN-like TCPs might prevent the dissection of leaf margins. The molecular basis for the action of CIN-like TCPs provides an insight into the temporal regulation of the complexity of leaf margins and explains the inability of *KNOX* genes to induce the dissection of the simplified leaves of the *la* mutant of tomato (Hareven et al., 1996; Ori et al., 2007).

The functional redundancy of *CIN*-like *TCP* genes and the indirect regulation of the expression of *CUC* genes by CIN-like TCPs might increase the robustness and flexibility of the regulatory process that governs leaf development. Functional redundancy protects regulatory processes from the possible disruptive effects of mutations (Gu et al., 2003; Chapman et al., 2006). The extreme redundancy of *CIN*-like *TCP* genes results in single mutations of *CIN*-like *TCP* genes having only subtle effects on the growth of *Arabidopsis* plants. The product of each of the individual direct target genes of TCP3 partially, and in cooperation with the others, represses the expression of *CUC* genes. Thus, we can understand why inactivation of one of the target genes has only a limited effect on the regulation of leaf development, as observed in single *as1*, *mir164*a, *iaa3*/*shy2*, and *saur* mutant plants (Tian and Reed, 1999; Byrne et al., 2000; Hagen and Guilfoyle, 2002; Nikovics et al., 2006). The functional redundancy of genes and the robustness of regulatory linkages allow the accumulation of nonlethal mutations and can serve as sources of novel morphologies (Kirschner and Gerhart, 1998; Moore and Purugganan, 2005). Therefore, we propose that *CIN*-like *TCP* genes specify spatial and temporal signals that have conferred flexibility on leaf form during evolution.

METHODS

Plant Materials and Growth Conditions

Arabidopsis thaliana ecotype Columbia-0 was used throughout this study unless otherwise indicated. The following mutant and transgenic lines were used: *tcp4-1* (GK_363H08; Rosso et al., 2003), *tcp4-2* (GK_350D01), *tcp10-1* (SALK_137205; Alonso et al., 2003), *tcp13-2* (GK_182B12), *tcp5-1* (SM_3_29639; Tissier et al., 1999; Efroni et al., 2008), *tcp3-1* (Koyama et al., 2007), *Pro35S:mTCP3* (Koyama et al., 2007), *mir319a*^{129} (Landsberg *erecta*; Nag et al., 2009), *as1-1* (CS3373; Byrne et al., 2000), *mir164a-4* (GK_867E03; Nikovics et al., 2006), *ProAS1:GUS* (Iwakawa et al., 2007), *PromiR164A:GUS* (Nikovics et al., 2006), *ProIAA3/SHY2:GUS* (Landsberg *erecta* Tian et al., 2002), and *cuc1-5* and *cuc3-105* (Hibara et al., 2006). Plants were grown under conditions of 16-h light and 8-h dark unless otherwise indicated. For the observation of seedlings, plants were grown on a plate supplemented with Murashige and Skoog (MS) salts, 5 g/L sucrose, and 0.5 g/L MES. Naphthalene acetic acid (Sigma-Aldrich) was dissolved in DMSO and added in the MS plate. For the observation of rosette leaves, plants were grown in soil. For growth of

plants in liquid culture, 10-d-old seedlings were transferred into a liquid medium that contained half-strength MS salts, 5 g/L sucrose, and 0.5 g/L MES for 36 h with gentle agitation under continuous light conditions. After preculture of plants in the liquid medium, chemicals that included DMSO, 5 μM (final) estradiol (Wako), or 1 μM (final) IAA (Sigma-Aldrich) were added at times specified in the text or individual figure legends. Methods of *Agrobacterium tumefaciens*–mediated transformation were described previously (Mitsuda et al., 2006).

Construction of Plasmids

To generate the plasmid *ProXVE:TCP3SRDX*, we cloned the coding sequence of *TCP3SRDX* (Koyama et al., 2007) into pER8, a vector for use in the XVE system (Zuo et al., 2000). To construct plasmids *ProDR5:GUS* and *ProAt1g29460:GUS*, we inserted a DNA fragment corresponding to the DR5 element and 2 kb of the 5′ upstream region of *At1g29460*, respectively, upstream of the *GUS* gene in pBI101 (Clontech). To generate *LUCIFERASE* (*LUC*) reporter genes, we inserted DNA fragments corresponding to 1 kb of the 5′ upstream region of *AS1*, *miR164A*, and *At1g29460*, respectively, upstream of the *LUC* gene, as described previously (Fujimoto et al., 2000). To generate the *TCP3* effector gene, we inserted the coding sequence of *TCP3* downstream of the cauliflower mosaic virus 35S promoter and the tobacco mosaic virus omega sequence (Fujimoto et al., 2000). Nucleotides in the 5′ upstream regions of *At1g29460*, *AS1*, and *miR164A* were changed by site-directed mutagenesis with appropriate sets of primers (see Supplemental Table 8 online). The coding regions of *AS1*, *miR164A*, *IAA3/SHY2*, and *At1g29460* were inserted, respectively, into pBCKH to generate constructs for the ectopic expression of each gene (Mitsuda et al., 2006). The *Pro35S:miR319A* construct was described previously (Koyama et al., 2007).

Analysis of Gene Expression

Total RNA was isolated from tissues by the Trizol method (Fujimoto et al., 2000) or with RNAeasy (Qiagen) and subjected to microarray analysis or first-strand cDNA synthesis with SuperScript III (Invitrogen).

The microarray experiments were performed using an Agilent *Arabidopsis* V3 (4x44k) microarray according to the manufacturer's instructions. Three or four biological replicates were tested in a two-color method. Spot signal values were calculated by Feature Extraction version 9.1 software supplied by Agilent. We defined the QC value as 1 when a spot passed the FeatNonUnifOL filter and as 2 when the spot further passed the FeatPopnOL filter. We defined the detection value as 1 when a spot passed the IsPosAndSignif filter and as 2 when the spot further passed the IsWellAboveBG. All signal values were divided by the median value among spots with QC = 2 to allow comparisons with other microarray data. Spot-to-gene conversion was accomplished based on a table provided by The Arabidopsis Information Resource (ftp://ftp.Arabidopsis.org/home/tair/Microarrays/Agilent/agilent_array_elements-2009-7-29.txt), except for A_84_P581183 probe corresponding to *CUC1*. The average values were used for genes corresponding to two or more probes. Genes with average QC value < 1.5 in the test sample or the reference sample were excluded from subsequent analyses. Only genes with average detection value ≥ 1.5 in the reference sample were analyzed when selecting downregulated genes. The P value of each gene was calculated by Welch's *t* test. To estimate the FDR, we calculated the Q-value from the P value using QVALUE software with default settings (Storey and Tibshirani, 2003) and selected downregulated (<0.5-fold) genes with P values < 0.05 (FDR was < 0.05 in both experiments). Fisher's exact test was performed by R software (http://www.r-project.org/).

RT-PCR was performed with gene-specific primers as shown in Supplemental Table 8 online. PCR was terminated after 24, 27, or 30 cycles to ensure that PCR was in the liner range, unless otherwise indicated.

Observation of GUS Activity and Histological Analysis

For detection of GUS activity, plants were submerged and incubated in a buffer that contained 50 mM sodium phosphate, pH 7.0, 1 mM potassium ferricyanide, and 1 mM 5-bromo-4-chloro-3-indolyl-β-D-glucuronide (Nacalai Tesque). Tissues were then immersed in ethanol to remove chlorophyll. For observation of the vasculature and the epidermal cells, plant tissues were rendered transparent as described previously (Aida et al., 1997). Microscopy observations were performed with Axioskop2 plus (Carl Ziess), MZ FL III (Leica), and ECLIPS E600 (Nikon) systems.

ChIP Assays

The TCP3-specific antibodies were raised in rabbits by immunizing them with a synthetic peptide that corresponded to 16 amino acid residues in the C terminus of TCP3 (see Supplemental Figure 10A online) and were purified with affinity chromatography on a column conjugated with the peptide (Peptide Institute).

For preparation of crude extracts of nuclei, 2-week-old plants were submerged in 1% formaldehyde for 10 min for cross-linking. Samples were then frozen, ground with liquid nitrogen, and suspended in extraction buffer I (0.4 M sucrose, 10 mM Tris, pH 8.0, 10 mM $MgCl_2$, 5 mM β-mercaptoethanol, and protease inhibitor cocktail without EDTA; Roche). The extract was filtrated and centrifuged at 4000 rpm for 20 min at 4°C. The pellet was suspended in extraction buffer II (0.25 M sucrose, 10 mM Tris, pH 8.0, 10 mM $MgCl_2$, 1% Triton X-100, 5 mM β-mercaptoethanol, and protease inhibitor cocktail without EDTA), and the suspension was centrifuged at 13,000 rpm for 10 min at 4°C. The resultant pellet was suspended in extraction buffer II and layered on top of an equal volume of extraction buffer III (1.7 M sucrose, 10 mM Tris, pH 8.0, 2 mM $MgCl_2$, 0.15% Triton X-100, 5 mM β-mercaptoethanol, and protease inhibitor cocktail without EDTA) and centrifuged at 13,000 rpm for 1 h at 4°C. The resultant pellet was suspended in lysis buffer (50 mM Tris, pH 8.0, 10 mM EDTA, and 1% SDS), and the resuspended chromatin was sonicated to yield small fragments with an average length of 0.2 to 2 kb, centered around 0.5 kb.

For immunoprecipitation of chromatin, the sonicated chromatin was diluted 10-fold with dilution buffer (1.1% Triton X-100, 1.2 mM EDTA, 16.7 mM Tris, pH 8.0, and 167 mM NaCl) and cleared by incubation with Dynabeads Protein G (Invitrogen) that had been blocked with salmon sperm DNA. The cleared solution of chromatin fragments was incubated with 2 μL TCP3-specific antibodies overnight at 4°C. Immunocomplexes were recovered by incubation with Dynabeads Protein G (Invitrogen) for 1 h at 4°C. After several washings, immunocomplexes were eluted with elution buffer (1% SDS and 0.1 M $NHCO_3$) and subjected to reverse cross-linking by incubation at 70°C overnight. The chromatin was purified by incubation with protease K (Invitrogen), phenol-chloroform extraction, and ethanol precipitation. The purified chromatin was subjected to PCR for 33, 36, or 39 cycles with sets of primers (see Supplemental Table 8 online) specific for the detection of genomic regions corresponding to the promoter and the control.

Assays of Transient Gene Expression

Effector, reporter, and reference plasmids were introduced transiently into rosette leaves by the particle bombardment method, and the relative activity of *LUC* was quantified as described elsewhere (Koyama et al., 2007).

Accession Numbers

Sequence data for from this article can be found in the Arabidopsis Genome Initiative database under the following accession numbers: TCP2,

At4g18390; TCP3, At1g53230; TCP4, At3g15030; TCP5, At5g60970; TCP10, At2g31070; TCP13, At3g02150; TCP17, At5g08070; TCP24, At1g30210; miR319A, AT4G23713; CUC1, At3g15170; CUC2, At5g53950; CUC3, At1g76420; LOB, At5g63090; AS1, At2g37630; miR164A, At2g47585; IAA3/SHY2, At1g04240; IAA4, At5g43700; LBD16, At2g42430; KNAT1, At4g08150; and TUB, At5g23860. The microarray data were submitted to the National Center for Biotechnology Information Gene Expression Omnibus (http://www.ncbi.nlm.nih.gov/geo/; GSE20705).

Supplemental Data

The following materials are available in the online version of this article.

Supplemental Figure 1. Schematic Diagram of the Structures of *CIN*-Like *TCP* Genes and the Sites of Insertion of T-DNA into the Respective Genes.

Supplemental Figure 2. Expression of *CIN*-Like *TCP* Genes in *tcp* Mutants.

Supplemental Figure 3. Delayed Flowering of *tcp3/4/5/10/13* Plants.

Supplemental Figure 4. Inflorescent Stem of *Pro35S:miR319A tcp3/4/5/10/13* Plants.

Supplemental Figure 5. Smooth Margin of Leaves and Down-regulation of *CUC2* in the *mir319a*^{129} Mutant.

Supplemental Figure 6. Cotyledons of *ProXVE:TCP3SRDX*, *ProXVE:TCP3SRDX cuc1*, and *ProXVE:TCP3SRDX cuc1 cuc3* Plants.

Supplemental Figure 7. Expression of *TCP3SRDX* and *LOB* after Induction by Estradiol.

Supplemental Figure 8. Expression of the Target Genes of TCP3 at 8 h after Induction of *TCP3SRDX*.

Supplemental Figure 9. Functional Categorization of Genes Downstream of TCP3 Based on Gene Ontology.

Supplemental Figure 10. Specificity of Antibodies against TCP3 Used in This Study.

Supplemental Figure 11. Expression of Auxin-Inducible Genes after Continuous Induction of *TCP3SRDX*.

Supplemental Figure 12. Expression of the Target Genes of TCP3 in *Pro35S:mTCP3* Plants.

Supplemental Table 1. Changes in Expression of Boundary-Specific Genes upon Expression of *TCP3SRDX* Determined by Microarray Analysis of *ProXVE:TCP3SRDX* Plants.

Supplemental Table 2. Genes Containing *cis*-Elements in Their 1000-bp Upstream Regions That Are Overrepresented in the Genes Downstream of TCP3.

Supplemental Table 3. Changes of the Expression of 24 Out of 78 Genes Encoding Auxin-Inducible Proteins upon Expression of *TCP3SRDX* Determined by Microarray Analysis of *ProXVE:TCP3SRDX* and *ProXVE:TCP3SRDX cuc1* Plants.

Supplemental Table 4. Changes in Expression of Genes for the IAA/AUX Family Determined by Microarray Analysis of *ProXVE:TCP3SRDX* and *ProXVE:TCP3SRDX cuc1* Plants.

Supplemental Table 5. Changes in Expression of Genes for the PIN Family Determined by Microarray Analysis of *ProXVE:TCP3SRDX* and *ProXVE:TCP3SRDX cuc1* Plants.

Supplemental Table 6. Changes in Expression of the Genes for Organ Morphogenesis Determined by Microarray Analysis of *ProXVE:TCP3SRDX* and *ProXVE:TCP3SRDX cuc1* Plants.

Supplemental Table 7. Changes in Expression of Genes That Control Developmental Timing upon Expression of *TCP3SRDX*.

Supplemental Table 8. Primers Used in This Study.

ACKNOWLEDGMENTS

We thank T. Jack, P. Laufs, C. Machida, J. Reed, M. Tasaka, the ABRC, GABI_KAT, and the Nottingham Arabidopsis Stock Centre for seeds; N.H. Chua and T. Guilfoyle for plasmids; F. Sato for enabling T.K. to accomplish this work in his laboratory; R. Terauchi for the ChIP protocol; M. Aida for helpful discussions; and Y. Kimura, A. Kuwazawa, Y. Takiguchi, and N. Ujiie for skilled technical assistance. This work was supported by a Kyoto University Start-Up Grant-in-Aid for young scientists to T.K.

Received March 31, 2010; revised October 14, 2010; accepted November 9, 2010; published November 30, 2010.

REFERENCES

Adenot, X., Elmayan, T., Lauressergues, D., Boutet, S., Bouché, N., Gasciolli, V., and Vaucheret, H. (2006). DRB4-dependent *TAS3 trans*-acting siRNAs control leaf morphology through AGO7. Curr. Biol. **16:** 927–932.

Aida, M., Ishida, T., Fukaki, H., Fujisawa, H., and Tasaka, M. (1997). Genes involved in organ separation in Arabidopsis: An analysis of the *cup-shaped cotyledon* mutant. Plant Cell **9:** 841–857.

Aida, M., Ishida, T., and Tasaka, M. (1999). Shoot apical meristem and cotyledon formation during Arabidopsis embryogenesis: Interaction among the *CUP-SHAPED COTYLEDON* and *SHOOT MERISTEMLESS* genes. Development **126:** 1563–1570.

Allen, E., Xie, Z., Gustafson, A.M., and Carrington, J.C. (2005). MicroRNA-directed phasing during *trans*-acting siRNA biogenesis in plants. Cell **121:** 207–221.

Alonso, J.M., et al. (2003). Genome-wide insertional mutagenesis of *Arabidopsis thaliana*. Science **301:** 653–657.

Alvarez, J.P., Goldshmidt, A., Efroni, I., Bowman, J.L., and Eshed, Y. (2009). The *NGATHA* distal organ development genes are essential for style specification in *Arabidopsis.* Plant Cell **21:** 1373–1393.

Barkoulas, M., Hay, A., Kougioumoutzi, E., and Tsiantis, M. (2008). A developmental framework for dissected leaf formation in the *Arabidopsis* relative *Cardamine hirsuta*. Nat. Genet. **40:** 1136–1141.

Benková, E., Michniewicz, M., Sauer, M., Teichmann, T., Seifertová, D., Jürgens, G., and Friml, J. (2003). Local, efflux-dependent auxin gradients as a common module for plant organ formation. Cell **115:** 591–602.

Berger, Y., Harpaz-Saad, S., Brand, A., Melnik, H., Sirding, N., Alvarez, J.P., Zinder, M., Samach, A., Eshed, Y., and Ori, N. (2009). The NAC-domain transcription factor GOBLET specifies leaflet boundaries in compound tomato leaves. Development **136:** 823–832.

Blein, T., Pulido, A., Vialette-Guiraud, A., Nikovics, K., Morin, H., Hay, A., Johansen, I.E., Tsiantis, M., and Laufs, P. (2008). A conserved molecular framework for compound leaf development. Science **322:** 1835–1839.

Bowman, J.L., and Floyd, S.K. (2008). Patterning and polarity in seed plant shoots. Annu. Rev. Plant Biol. **59:** 67–88.

Brewer, P.B., Howles, P.A., Dorian, K., Griffith, M.E., Ishida, T., Kaplan-Levy, R.N., Kilinc, A., and Smyth, D.R. (2004). *PETAL LOSS*, a trihelix transcription factor gene, regulates perianth architecture in the *Arabidopsis* flower. Development **131:** 4035–4045.

Byrne, M.E., Barley, R., Curtis, M., Arroyo, J.M., Dunham, M., Hudson, A., and Martienssen, R.A. (2000). *Asymmetric leaves1* mediates leaf patterning and stem cell function in *Arabidopsis*. Nature **408:** 967–971.

Carraro, N., Peaucelle, A., Laufs, P., and Traas, J. (2006). Cell differentiation and organ initiation at the shoot apical meristem. Plant Mol. Biol. **60:** 811–826.

Caruso, J.L. (1968). Morphogenic aspects of a leafless mutant in tomato. General patterns of development. Am. J. Bot. **55:** 1169–1176.

Champagne, C., and Sinha, N. (2004). Compound leaves: Equal to the sum of their parts? Development **131:** 4401–4412.

Chapman, B.A., Bowers, J.E., Feltus, F.A., and Paterson, A.H. (2006). Buffering of crucial functions by paleologous duplicated genes may contribute cyclicality to angiosperm genome duplication. Proc. Natl. Acad. Sci. USA **103:** 2730–2735.

Cheng, Y., Dai, X., and Zhao, Y. (2006). Auxin biosynthesis by the YUCCA flavin monooxygenases controls the formation of floral organs and vascular tissues in *Arabidopsis*. Genes Dev. **20:** 1790–1799.

Cheng, Y., Qin, G., Dai, X., and Zhao, Y. (2008). *NPY* genes and AGC kinases define two key steps in auxin-mediated organogenesis in *Arabidopsis*. Proc. Natl. Acad. Sci. USA **105:** 21017–21022.

Dello Ioio, R., Nakamura, K., Moubayidin, L., Perilli, S., Taniguchi, M., Morita, M.T., Aoyama, T., Costantino, P., and Sabatini, S. (2008). A genetic framework for the control of cell division and differentiation in the root meristem. Science **322:** 1380–1384.

Efroni, I., Blum, E., Goldshmidt, A., and Eshed, Y. (2008). A protracted and dynamic maturation schedule underlies *Arabidopsis* leaf development. Plant Cell **20:** 2293–2306.

Fahlgren, N., Montgomery, T.A., Howell, M.D., Allen, E., Dvorak, S.K., Alexander, A.L., and Carrington, J.C. (2006). Regulation of *AUXIN RESPONSE FACTOR3* by *TAS3* ta-siRNA affects developmental timing and patterning in *Arabidopsis*. Curr. Biol. **16:** 939–944.

Fujimoto, S.Y., Ohta, M., Usui, A., Shinshi, H., and Ohme-Takagi, M. (2000). Arabidopsis ethylene-responsive element binding factors act as transcriptional activators or repressors of GCC box-mediated gene expression. Plant Cell **12:** 393–404.

Furutani, M., Vernoux, T., Traas, J., Kato, T., Tasaka, M., and Aida, M. (2004). *PIN-FORMED1* and *PINOID* regulate boundary formation and cotyledon development in Arabidopsis embryogenesis. Development **131:** 5021–5030.

Garcia, D., Collier, S.A., Byrne, M.E., and Martienssen, R.A. (2006). Specification of leaf polarity in *Arabidopsis* via the *trans*-acting siRNA pathway. Curr. Biol. **16:** 933–938.

Gu, Z., Steinmetz, L.M., Gu, X., Scharfe, C., Davis, R.W., and Li, W.H. (2003). Role of duplicate genes in genetic robustness against null mutations. Nature **421:** 63–66.

Guo, M., Thomas, J., Collins, G., and Timmermans, M.C. (2008). Direct repression of KNOX loci by the ASYMMETRIC LEAVES1 complex of *Arabidopsis*. Plant Cell **20:** 48–58.

Hagen, G., and Guilfoyle, T. (2002). Auxin-responsive gene expression: Genes, promoters and regulatory factors. Plant Mol. Biol. **49:** 373–385.

Hake, S., Smith, H.M., Holtan, H., Magnani, E., Mele, G., and Ramirez, J. (2004). The role of *knox* genes in plant development. Annu. Rev. Cell Dev. Biol. **20:** 125–151.

Hamann, T., Benkova, E., Bäurle, I., Kientz, M., and Jürgens, G. (2002). The Arabidopsis *BODENLOS* gene encodes an auxin response protein inhibiting *MONOPTEROS*-mediated embryo patterning. Genes Dev. **16:** 1610–1615.

Hareven, D., Gutfinger, T., Parnis, A., Eshed, Y., and Lifschitz, E. (1996). The making of a compound leaf: Genetic manipulation of leaf architecture in tomato. Cell **84:** 735–744.

Hay, A., Barkoulas, M., and Tsiantis, M. (2006). ASYMMETRIC LEAVES1 and auxin activities converge to repress *BREVIPEDICELLUS* expression and promote leaf development in Arabidopsis. Development **133:** 3955–3961.

Hay, A., Kaur, H., Phillips, A., Hedden, P., Hake, S., and Tsiantis, M. (2002). The gibberellin pathway mediates KNOTTED1-type homeobox function in plants with different body plans. Curr. Biol. **12:** 1557–1565.

Hay, A., and Tsiantis, M. (2006). The genetic basis for differences in leaf form between *Arabidopsis thaliana* and its wild relative *Cardamine hirsuta*. Nat. Genet. **38:** 942–947.

Heisler, M.G., Ohno, C., Das, P., Sieber, P., Reddy, G.V., Long, J.A., and Meyerowitz, E.M. (2005). Patterns of auxin transport and gene expression during primordium development revealed by live imaging of the *Arabidopsis* inflorescence meristem. Curr. Biol. **15:** 1899–1911.

Hibara, K., Karim, M.R., Takada, S., Taoka, K., Furutani, M., Aida, M., and Tasaka, M. (2006). *Arabidopsis CUP-SHAPED COTYLEDON3* regulates postembryonic shoot meristem and organ boundary formation. Plant Cell **18:** 2946–2957.

Hibara, K., Takada, S., and Tasaka, M. (2003). *CUC1* gene activates the expression of SAM-related genes to induce adventitious shoot formation. Plant J. **36:** 687–696.

Hiratsu, K., Matsui, K., Koyama, T., and Ohme-Takagi, M. (2003). Dominant repression of target genes by chimeric repressors that include the EAR motif, a repression domain, in *Arabidopsis*. Plant J. **34:** 733–739.

Hu, Y., Xie, Q., and Chua, N.H. (2003). The Arabidopsis auxin-inducible gene *ARGOS* controls lateral organ size. Plant Cell **15:** 1951–1961.

Hunter, C., Sun, H., and Poethig, R.S. (2003). The *Arabidopsis* heterochronic gene *ZIPPY* is an *ARGONAUTE* family member. Curr. Biol. **13:** 1734–1739.

Hunter, C., Willmann, M.R., Wu, G., Yoshikawa, M., de la Luz Gutiérrez-Nava, M., and Poethig, S.R. (2006). Trans-acting siRNA-mediated repression of ETTIN and ARF4 regulates heteroblasty in Arabidopsis. Development **133:** 2973–2981.

Iwakawa, H., Iwasaki, M., Kojima, S., Ueno, Y., Soma, T., Tanaka, H., Semiarti, E., Machida, Y., and Machida, C. (2007). Expression of the *ASYMMETRIC LEAVES2* gene in the adaxial domain of Arabidopsis leaves represses cell proliferation in this domain and is critical for the development of properly expanded leaves. Plant J. **51:** 173–184.

Izhaki, A., and Bowman, J.L. (2007). KANADI and class III HD-Zip gene families regulate embryo patterning and modulate auxin flow during embryogenesis in *Arabidopsis*. Plant Cell **19:** 495–508.

Kant, S., Bi, Y.M., Zhu, T., and Rothstein, S.J. (2009). *SAUR39*, a small auxin-up RNA gene, acts as a negative regulator of auxin synthesis and transport in rice. Plant Physiol. **151:** 691–701.

Kirschner, M., and Gerhart, J. (1998). Evolvability. Proc. Natl. Acad. Sci. USA **95:** 8420–8427.

Koenig, D., Bayer, E., Kang, J., Kuhlemeier, C., and Sinha, N. (2009). Auxin patterns *Solanum lycopersicum* leaf morphogenesis. Development **136:** 2997–3006.

Kosugi, S., and Ohashi, Y. (2002). DNA binding and dimerization specificity and potential targets for the TCP protein family. Plant J. **30:** 337–348.

Koyama, T., Furutani, M., Tasaka, M., and Ohme-Takagi, M. (2007). TCP transcription factors control the morphology of shoot lateral organs via negative regulation of the expression of boundary-specific genes in *Arabidopsis*. Plant Cell **19:** 473–484.

Kumar, R., Kushalappa, K., Godt, D., Pidkowich, M.S., Pastorelli, S., Hepworth, S.R., and Haughn, G.W. (2007). The *Arabidopsis* BEL1-LIKE HOMEODOMAIN proteins SAW1 and SAW2 act redundantly to regulate *KNOX* expression spatially in leaf margins. Plant Cell **19:** 2719–2735.

Larue, C.T., Wen, J., and Walker, J.C. (2009). A microRNA-transcription factor module regulates lateral organ size and patterning in *Arabidopsis*. Plant J. **58:** 450–463.

Laux, T., Würschum, T., and Breuninger, H. (2004). Genetic regulation of embryonic pattern formation. Plant Cell **16** (suppl.): S190–S202.

Liscum, E., and Reed, J.W. (2002). Genetics of Aux/IAA and ARF action in plant growth and development. Plant Mol. Biol. **49:** 387–400.

Martín-Trillo, M., and Cubas, P. (2010). TCP genes: A family snapshot ten years later. Trends Plant Sci. **15:** 31–39.

Mathan, D., and Jenkins, J. (1962). A morphogenic study of *lanceolate*, a leaf-shape mutant in the tomato. Am. J. Bot. **49:** 504–514.

Mitsuda, N., Hiratsu, K., Todaka, D., Nakashima, K., Yamaguchi-Shinozaki, K., and Ohme-Takagi, M. (2006). Efficient production of male and female sterile plants by expression of a chimeric repressor in Arabidopsis and rice. Plant Biotechnol. J. **4:** 325–332.

Moore, R.C., and Purugganan, M.D. (2005). The evolutionary dynamics of plant duplicate genes. Curr. Opin. Plant Biol. **8:** 122–128.

Nag, A., King, S., and Jack, T. (2009). miR319a targeting of TCP4 is critical for petal growth and development in Arabidopsis. Proc. Natl. Acad. Sci. USA **106:** 22534–22539.

Nath, U., Crawford, B.C., Carpenter, R., and Coen, E. (2003). Genetic control of surface curvature. Science **299:** 1404–1407.

Nikovics, K., Blein, T., Peaucelle, A., Ishida, T., Morin, H., Aida, M., and Laufs, P. (2006). The balance between the *MIR164A* and *CUC2* genes controls leaf margin serration in *Arabidopsis*. Plant Cell **18:** 2929–2945.

Okushima, Y., Fukaki, H., Onoda, M., Theologis, A., and Tasaka, M. (2007). ARF7 and ARF19 regulate lateral root formation via direct activation of *LBD*/*ASL* genes in *Arabidopsis*. Plant Cell **19:** 118–130.

Ori, N., et al. (2007). Regulation of *LANCEOLATE* by *miR319* is required for compound-leaf development in tomato. Nat. Genet. **39:** 787–791.

Ori, N., Eshed, Y., Chuck, G., Bowman, J.L., and Hake, S. (2000). Mechanisms that control *knox* gene expression in the *Arabidopsis* shoot. Development **127:** 5523–5532.

Palatnik, J.F., Allen, E., Wu, X., Schommer, C., Schwab, R., Carrington, J.C., and Weigel, D. (2003). Control of leaf morphogenesis by microRNAs. Nature **425:** 257–263.

Phelps-Durr, T.L., Thomas, J., Vahab, P., and Timmermans, M.C. (2005). Maize rough sheath2 and its *Arabidopsis* orthologue ASYMMETRIC LEAVES1 interact with HIRA, a predicted histone chaperone, to maintain *knox* gene silencing and determinacy during organogenesis. Plant Cell **17:** 2886–2898.

Reiser, L., Modrusan, Z., Margossian, L., Samach, A., Ohad, N., Haughn, G.W., and Fischer, R.L. (1995). The *BELL1* gene encodes a homeodomain protein involved in pattern formation in the Arabidopsis ovule primordium. Cell **83:** 735–742.

Rosso, M.G., Li, Y., Strizhov, N., Reiss, B., Dekker, K., and Weisshaar, B. (2003). An *Arabidopsis thaliana* T-DNA mutagenized population (GABI-Kat) for flanking sequence tag-based reverse genetics. Plant Mol. Biol. **53:** 247–259.

Scarpella, E., Marcos, D., Friml, J., and Berleth, T. (2006). Control of leaf vascular patterning by polar auxin transport. Genes Dev. **20:** 1015–1027.

Schneeberger, R., Tsiantis, M., Freeling, M., and Langdale, J.A. (1998). The *rough sheath2* gene negatively regulates homeobox gene expression during maize leaf development. Development **125:** 2857–2865.

Schommer, C., Palatnik, J.F., Aggarwal, P., Chételat, A., Cubas, P., Farmer, E.E., Nath, U., and Weigel, D. (2008). Control of jasmonate biosynthesis and senescence by miR319 targets. PLoS Biol. **6:** e230.

Semiarti, E., Ueno, Y., Tsukaya, H., Iwakawa, H., Machida, C., and Machida, Y. (2001). The *ASYMMETRIC LEAVES2* gene of *Arabidopsis thaliana* regulates formation of a symmetric lamina, establishment of venation and repression of meristem-related homeobox genes in leaves. Development **128:** 1771–1783.

Settler, R. (1964). Dosage effects of the *Lanceolate* gene in tomato. Am. J. Bot. **51:** 253–264.

Sieber, P., Wellmer, F., Gheyselinck, J., Riechmann, J.L., and Meyerowitz, E.M. (2007). Redundancy and specialization among plant microRNAs: Role of the *MIR164* family in developmental robustness. Development **134:** 1051–1060.

Storey, J.D., and Tibshirani, R. (2003). Statistical significance for genomewide studies. Proc. Natl. Acad. Sci. USA **100:** 9440–9445.

Tian, Q., and Reed, J.W. (1999). Control of auxin-regulated root development by the *Arabidopsis thaliana SHY2/IAA3* gene. Development **126:** 711–721.

Tian, Q., Uhlir, N.J., and Reed, J.W. (2002). Arabidopsis SHY2/IAA3 inhibits auxin-regulated gene expression. Plant Cell **14:** 301–319.

Timmermans, M.C., Hudson, A., Becraft, P.W., and Nelson, T. (1999). ROUGH SHEATH2: A Myb protein that represses *knox* homeobox genes in maize lateral organ primordia. Science **284:** 151–153.

Tissier, A.F., Marillonnet, S., Klimyuk, V., Patel, K., Torres, M.A., Murphy, G., and Jones, J.D. (1999). Multiple independent defective *suppressor-mutator* transposon insertions in Arabidopsis: A tool for functional genomics. Plant Cell **11:** 1841–1852.

Trigueros, M., Navarrete-Gómez, M., Sato, S., Christensen, S.K., Pelaz, S., Weigel, D., Yanofsky, M.F., and Ferrándiz, C. (2009). The *NGATHA* genes direct style development in the *Arabidopsis* gynoecium. Plant Cell **21:** 1394–1409.

Tsiantis, M., Schneeberger, R., Golz, J.F., Freeling, M., and Langdale, J.A. (1999). The maize *rough sheath2* gene and leaf development programs in monocot and dicot plants. Science **284:** 154–156.

Tsukaya, H. (2005). Leaf shape: Genetic controls and environmental factors. Int. J. Dev. Biol. **49:** 547–555.

Ueno, Y., Ishikawa, T., Watanabe, K., Terakura, S., Iwakawa, H., Okada, K., Machida, C., and Machida, Y. (2007). Histone deacetylases and ASYMMETRIC LEAVES2 are involved in the establishment of polarity in leaves of *Arabidopsis*. Plant Cell **19:** 445–457.

Ulmasov, T., Murfett, J., Hagen, G., and Guilfoyle, T.J. (1997). Aux/IAA proteins repress expression of reporter genes containing natural and highly active synthetic auxin response elements. Plant Cell **9:** 1963–1971.

Vroemen, C.W., Mordhorst, A.P., Albrecht, C., Kwaaitaal, M.A., and de Vries, S.C. (2003). The *CUP-SHAPED COTYLEDON3* gene is required for boundary and shoot meristem formation in Arabidopsis. Plant Cell **15:** 1563–1577.

Waites, R., Selvadurai, H.R., Oliver, I.R., and Hudson, A. (1998). The *PHANTASTICA* gene encodes a MYB transcription factor involved in growth and dorsoventrality of lateral organs in *Antirrhinum*. Cell **93:** 779–789.

Weigel, D., and Jürgens, G. (2002). Stem cells that make stems. Nature **415:** 751–754.

Weijers, D., Benkova, E., Jäger, K.E., Schlereth, A., Hamann, T., Kientz, M., Wilmoth, J.C., Reed, J.W., and Jürgens, G. (2005). Developmental specificity of auxin response by pairs of ARF and Aux/IAA transcriptional regulators. EMBO J. **24:** 1874–1885.

Xu, B., Li, Z., Zhu, Y., Wang, H., Ma, H., Dong, A., and Huang, H. (2008). Arabidopsis genes *AS1, AS2*, and *JAG* negatively regulate boundary-specifying genes to promote sepal and petal development. Plant Physiol. **146:** 566–575.

Zuo, J., Niu, Q.W., and Chua, N.H. (2000). Technical advance: An estrogen receptor-based transactivator XVE mediates highly inducible gene expression in transgenic plants. Plant J. **24:** 265–273.

TCP Transcription Factors Regulate the Activities of ASYMMETRIC LEAVES1 and miR164, as Well as the Auxin Response, during Differentiation of Leaves in *Arabidopsis*
Tomotsugu Koyama, Nobutaka Mitsuda, Motoaki Seki, Kazuo Shinozaki and Masaru Ohme-Takagi
Plant Cell 2010;22;3574-3588; originally published online November 30, 2010;
DOI 10.1105/tpc.110.075598

This information is current as of July 19, 2018

Supplemental Data	**/content/suppl/2010/11/10/tpc.110.075598.DC1.html**
References	This article cites 88 articles, 50 of which can be accessed free at: /content/22/11/3574.full.html#ref-list-1
Permissions	https://www.copyright.com/ccc/openurl.do?sid=pd_hw1532298X&issn=1532298X&WT.mc_id=pd_hw1532298X
eTOCs	Sign up for eTOCs at: http://www.plantcell.org/cgi/alerts/ctmain
CiteTrack Alerts	Sign up for CiteTrack Alerts at: http://www.plantcell.org/cgi/alerts/ctmain
Subscription Information	Subscription Information for *The Plant Cell* and *Plant Physiology* is available at: http://www.aspb.org/publications/subscriptions.cfm

© American Society of Plant Biologists
ADVANCING THE SCIENCE OF PLANT BIOLOGY